

Inelastic Electron-Deuteron Scattering Cross Sections at High Energies. II. Final-State Interactions and Relativistic Corrections*

LOYAL DURAND, III†

Brookhaven National Laboratory, Upton, New York

(Received March 30, 1961; revised manuscript received May 11, 1961)

Measurements of the cross-section $d^2\sigma/(d\Omega_e dE_e')$ for the inelastic electron-deuteron scattering process $e+d \rightarrow e+n+p$ have been used to determine the electromagnetic structure of the neutron. The effects on the theoretical cross section of interactions between the outgoing nucleons are examined in detail using the methods of a previous paper. The transition matrix elements connecting the initial state of the two-nucleon system (the deuteron) to a final state with specified total, orbital, and spin angular momenta are calculated using approximate wave functions which are matched to the experimentally determined neutron-proton scattering phase shifts. While individual matrix elements may be drastically changed by the distortion of the final-state wave functions by the neutron-proton interaction, the over-all corrections to the peak value of the cross section are found to be small (-1 to -2%) for electron momentum transfers in the range $q=3.4-2.6 \text{ f}^{-1}$. The precise magnitude of the corrections is somewhat uncertain because of the approximate nature of the wave functions, but it is unlikely either that they are large, or that the corrections could become positive. The effects of final-state interactions on the cross-section $d^2\sigma/(d\Omega_e dE_e')$ are also examined for final electron energies near the upper limit of the inelastic continuum. In this region, the nucleons emerge with low relative momenta, and, in agreement of the predictions of Jankus, the cross section is found to be drastically changed by the strong interactions in the final S states. However, it is shown that the presence in the neutron-proton interaction of a strongly repulsive

core results in a considerable diminution of the cross section relative to the predictions of Jankus for large values of q . This lowering of the cross section has been observed by Kendall *et al.* Results obtained with approximate repulsive core wave functions provide a reasonable fit both to the inelastic cross section near the end point, and to the deuteron electromagnetic form factor obtained from elastic electron-deuteron scattering. Finally, the relativistic theory of inelastic electron-deuteron scattering is examined using the methods of dispersion relations. It is found that in the region of the large peak, the cross-section $d^2\sigma/(d\Omega_e dE_e')$ is given essentially correctly by a nonrelativistic calculation using a modified Hamiltonian, provided the results are interpreted correctly with respect to the kinematics. The approximations inherent in the calculation are examined in detail. The resulting cross section differs significantly from the modified Jankus cross section which has been used in the analysis of the high-energy electron-deuteron scattering data obtained by the Stanford group. It is found that the apparent values of the neutron charge form factor F_{1n} are reduced essentially to zero for q^2 in the range $5 \text{ f}^{-2} \leq q^2 \leq 20 \text{ f}^{-2}$ when relativistic corrections, the effects of the deuteron D -states scattering, and the effects of final-state interactions are taken into account. Corresponding reductions in the value of the neutron anomalous magnetic moment form factor F_{2n} range up to about 30%, and bring F_{2n} into closer agreement with F_{2p} . A complete re-analysis of the experimental data will be necessary.

INTRODUCTION

CONSIDERABLE effort has been devoted in recent years to the determination of the structure of the neutron and the proton as reflected in the electromagnetic interactions of those particles. In particular, the high-energy electron-proton scattering experiments of Hofstadter¹ and Wilson² and their co-workers provide a direct measurement of the charge and anomalous magnetic moment form factors $F_{1p}(q^2)$ and $F_{2p}(q^2)$ which appear in the matrix element of the proton electromagnetic current operator,³

$$\langle p' | j_\mu | p \rangle = -ie\bar{u}(p') [F_{1p}\gamma_\mu + (\kappa_p/2m)F_{2p}\sigma_{\mu\nu}(p'-p)_\nu] u(p).$$

[Here κ_p is the anomalous part of the proton magnetic moment, m is the proton mass, and $q=p'-p$ is the 4-momentum transferred to the proton.] Information on the corresponding form factors $F_{1n}(q^2)$ and $F_{2n}(q^2)$

for the neutron charge and anomalous magnetic moment distributions has been obtained by using the deuteron as a source of "quasi-free" neutrons. However, the interpretation in terms of free-particle form factors of the high-energy inelastic electron-deuteron scattering cross sections measured by the Stanford⁴ and Cornell⁵ groups, and of the elastic scattering cross sections measured at Stanford,^{6,7} is considerably complicated by the presence of the extra nucleon in the deuteron. Thus the determination of the nucleon form factors at large values of q^2 using the measured elastic scattering cross sections requires detailed knowledge about the behavior of the deuteron wave function for small separations between the nucleons. Friedman *et al.*⁷ have suggested that this difficulty may be circumvented by considering the ratio of the cross sections for large and small electron scattering angles at a fixed value of q^2 . On the basis of the nonrelativistic theory of Jankus,⁸ this ratio should

* Work performed under the auspices of the U. S. Atomic Energy Commission.

† Now at Yale University, New Haven, Connecticut.

¹ E. E. Chambers and R. Hofstadter, Phys. Rev. **103**, 1454 (1956).

² F. Bumiller, N. Croissiaux, and R. Hofstadter, Phys. Rev. Letters, **5**, 261 (1960); R. Hofstadter, F. Bumiller, and M. Croissiaux, *ibid.* **5**, 263 (1960); R. R. Wilson, K. Berkman, J. M. Cassels, and D. N. Olson, Nature **188**, 94 (1960).

³ See, for example, the discussion of the nucleon form factors given by D. R. Yennie, M. M. Lévy, and D. G. Ravenhall, Revs. Modern Phys. **29**, 144 (1957).

⁴ M. R. Yearian and R. Hofstadter, Phys. Rev. **110**, 552 (1958); **111**, 934, (1958). S. Sobottka, *ibid.* **118**, 831 (1960). R. Hofstadter, C. deVries, and R. Herman, Phys. Rev. Letters **6**, 290 (1961). R. Hofstadter and R. Herman, *ibid.* **6**, 293 (1961).

⁵ D. N. Olson, H. F. Schopper, and R. R. Wilson, Phys. Rev. Letters **6**, 286 (1961).

⁶ J. McIntyre and R. Hofstadter, Phys. Rev. **98**, 158 (1956). J. McIntyre, *ibid.* **103**, 1464 (1956). J. McIntyre and S. Dhar, *ibid.* **106**, 1074 (1957). J. McIntyre and G. Burleson, *ibid.* **112**, 2077 (1958).

⁷ J. I. Friedman, H. W. Kendall, and P. A. M. Gram, III, Phys. Rev. **120**, 992 (1960).

⁸ V. Z. Jankus, Phys. Rev. **102**, 1586 (1956).

depend only on the form factors for free nucleons.⁷ It is not clear that this would be the case in the relativistic theory, since for large values of q^2 , the contributions to the scattering of mesonic currents within the deuteron are expected to be large. It should furthermore be noted that the nucleons are in this case considerably off the mass shell, so that the measured form factors may differ significantly from those for free nucleons. The theoretical situation is considerably more favorable for inelastic electron-deuteron scattering if the final electron energies are restricted to the region of the large peak which corresponds to quasi-elastic scattering from a single nucleon. Less detailed knowledge about the deuteron wave function is required than in the case of elastic scattering, the nucleons being on the average rather far apart. Mesonic corrections to the cross section are therefore expected to be rather small, and the nucleons are nearly on the mass shell. A number of relativistic corrections can furthermore be calculated quite easily. The major new complication is the presence of strong interactions between the outgoing nucleons.

The basic nonrelativistic theory of inelastic electron-deuteron scattering was given by Jankus,⁸ who calculated the cross-section $d^2\sigma/(d\Omega dE_e')$ using a Hulthén S -state model for the deuteron wave function, and plane waves for the wave functions of the outgoing nucleons. The effect on the cross section of interactions between the outgoing nucleons was considered approximately, using a central force model for the two-nucleon interaction, and treating its effect on the final nucleon wave functions in first Born approximation. The change in $d^2\sigma/(d\Omega dE_e')$ in the region of the quasi-elastic peak was found to be negligible. However, very large final state effects were shown to exist for final electron energies and scattering angles such that the neutron and proton emerged predominantly in the 3S_1 and 1S_0 states with low relative momenta. A more complete formulation of the problem of calculating final state effects was given by the present author in a paper in which relativistic corrections to the work of Jankus and the influence of the D -state component of the deuteron wave function on the scattering were also considered.⁹ Rough estimates made at that time indicated that the corrections to the cross section resulting from final-state interactions could be much larger than estimated by Jankus,⁸ decreasing the theoretical value of the cross section at the quasi-elastic peak by perhaps 5% or more. Because electron scattering from the neutron contributes only a small part of the peak value of $d^2\sigma/(d\Omega dE_e')$ for most of the values of q so far studied, an error of a few percent in the theoretical value of the cross section may alter appreciably the value of the neutron form factors obtained by matching the theoretical to the experimental cross section. It is, therefore, of some interest to consider these effects more thoroughly. In addition, recent

experimental results of Kendall *et al.*¹⁰ on the cross-section $d^2\sigma/(d\Omega dE_e')$ do not agree well with the simple Jankus theory in the region in which large effects resulting from interactions in the 3S_1 and 1S_0 final states are present, suggesting that previous calculations of these effects be re-examined.

In Sec. I of the present paper the principal results of (I)⁹ concerning the treatment of final state interactions will be reviewed, and the final results for the cross-section $d^2\sigma/(d\Omega dE_e')$ in the presence of such interactions will be recast in a form more amenable to numerical calculations. A set of approximate calculations of the effects of final state interactions on the peak cross section will be discussed in Sec. II. Despite the changes in the contributions of individual final states of the neutron-proton system to the cross section considerably larger than previously estimated,⁹ the overall change in the peak value of the cross section is found to be small. The theoretical value of $d^2\sigma/(d\Omega dE_e')$ is decreased by $\sim 2.2\%$ for an initial electron energy of 500 Mev, a scattering angle $\theta = 75^\circ$ in the laboratory system, and a momentum transfer $q = 2.6 \text{ f}^{-1}$. For $E_e = 500 \text{ Mev}$, $\theta = 135^\circ$, and $q = 3.4 \text{ f}^{-1}$, the cross section is again decreased, but by only $\sim 0.9\%$. These calculations are based on approximate wave functions for the final state of the two-nucleon system, but wave functions which are matched to the experimental values of the neutron-proton scattering phase shifts. It is therefore believed that the present results are at least indicative of those which would be found using wave functions calculated from one of the semi-phenomenological potentials which fit the scattering data. In Sec. III, the effects of final state interactions on the cross-section $d^2\sigma/(d\Omega dE_e')$ near the threshold for deuteron breakup will be examined. It will be shown that the discrepancies between the Jankus theory⁸ and the experiments of Kendall *et al.*¹⁰ can be attributed to the presence of a hard core in the neutron-proton interaction in the 3S_1 and 1S_0 states. Repulsive-core wave functions matched to the low-energy neutron-proton scattering data and the measured deuteron form factor are found to give a reasonable fit to the data, but the calculations presented are again primarily exploratory in character. It is nevertheless evident that a careful study of the inelastic scattering cross section near threshold can yield important information about the structure of the 3S_1 and 1S_0 wave functions of the neutron-proton system for small internucleon separations. Calculation of the necessary matrix elements using wave functions obtained from the semiphenomenological two-nucleon potentials which fit the high-energy neutron-proton scattering data would therefore be of considerable interest.

⁹ Loyal Durand, III, Phys. Rev. **115**, 1020 (1959); referred to hereafter as (I).

¹⁰ H. W. Kendall, J. I. Friedman, and P. A. M. Gram, III, Bull. Am. Phys. Soc. **5**, 270 (1960). The author would like to thank Professor Kendall for sending him details of the measurements of the inelastic cross sections near threshold.

The calculations of the preceding sections are based on a semirelativistic Hamiltonian for the interaction of the nucleons with the electromagnetic field of the scattered electron, but the wave functions for the initial and final states of the two-nucleon system are treated non-relativistically. Relativistic corrections are considered in Sec. IV using the methods of dispersion relations; this discussion of relativistic effects extends considerably that given in (I). In particular, it is shown that, in the absence of final-state interactions, the semirelativistic results for the peak cross section agree with those of the relativistic theory except for a kinematical factor and other relatively small corrections when the electron 3-momentum transfer in the laboratory system is replaced by the 3-momentum transfer in the center-of-mass system of the outgoing nucleons. Calculation of the effects of final state interactions would require an examination of the double spectral function in the Mandelstam representation for the transition matrix element. Anomalous thresholds are present in the double dispersion relations, and it appears likely that the spectral function in the anomalous region can be related to the nonrelativistic wave functions. However, no detailed calculations have been undertaken because of the smallness of the effects of final-state interactions indicated by the semirelativistic calculations of Sec. II. The situation is more complicated for the cross section near the threshold for deuteron breakup. Final-state interactions are very important, as was noted by Jankus,⁸ and one may also expect relativistic and mesonic corrections to the simple theory to be large. A detailed calculation of these effects would be of considerable interest, but is not undertaken here.

The present situation with respect to the theory of inelastic electron-deuteron scattering is summarized in Sec. V, and the effects of the known corrections to the cross section on the determination of the neutron form factors are examined. It is found that relativistic correction to the cross section, the effects of final-state interactions, and the corrections for scattering involving the deuteron D state, lead to large systematic changes in the values of the neutron form factors⁴ obtained from the experimental cross-sections $d^2\sigma/(d\Omega_e dE_e')$ on the basis of the modified Jankus theory.^{4,8} The neutron charge form factor F_{1n} is greatly reduced in value for q^2 in the range $5 \text{ f}^{-2} \leq q^2 \leq 20 \text{ f}^{-2}$; it is consistent with the present results to have $F_{1n} \approx 0$ in this range, contrary to the conclusions based on the Jankus cross section.⁴ The corresponding reductions in the value of the anomalous magnetic moment form factor are somewhat smaller, ranging up to 30%, and bring F_{2n} into closer agreement with F_{2p} . A complete reanalysis of the experimental data will be necessary, but has not yet been completed. The results of the exploratory calculations are summarized in Table VI.

I. THEORY OF FINAL-STATE EFFECTS

The theory of the inelastic electron-deuteron scattering process $e+d \rightarrow e+n+p$ including the effects of interactions between the outgoing nucleons was developed in detail in a previous paper (I).⁹ We will here be concerned with the cross-section $d^2\sigma/(d\Omega_e dE_e')$ for the scattering of an electron of initial energy E_e through an angle θ into the element of solid angle $d\Omega_e$, the electron having finally an energy in the interval dE_e' about the energy E_e' . All the foregoing quantities are to be measured in the deuteron rest system (laboratory system). The desired cross section is obtained by integrating over the direction of emission of the nucleons in their center-of-mass system the cross-section $d^3\sigma/(d\Omega_p d\Omega_n dE_e')$, and depends, therefore, on the final center-of-mass momentum of the nucleons, but not on their angular distribution. The necessary kinematic relations are easily derived. The 4-momentum q transferred from the electron to the neutron-proton system in the scattering is given in units with $\hbar=c=1$ by

$$q^2 = 4E_e E_e' \sin^2(\frac{1}{2}\theta), \quad (1)$$

while the momentum $p = |\mathbf{p}|$ of either of the nucleons in their final center-of-mass system is connected to the electron energies and the scattering angle by

$$p^2 = m(E_e - E_e' - \epsilon) - \frac{1}{4}q^2. \quad (2)$$

Here m is the nucleon mass, and $\epsilon = 2.226 \text{ Mev}$ is the deuteron binding energy. The cross-section $d^2\sigma/(d\Omega_e dE_e')$ has a threshold for a fixed incident energy E_e and a scattering angle θ at the value of E_e' for which the emerging nucleons are free, but have zero relative momentum, $p=0$. Combining Eqs. (1) and (2), the threshold value E_0 of E_e' is seen to be

$$E_0 = (E_e - \epsilon)[1 + (E_e/m) \sin^2(\frac{1}{2}\theta)]^{-1}. \quad (3)$$

For comparison, the electron can scatter elastically from the deuteron at an energy

$$(E_e')_{el} = E_e[1 + (E_e/m) \sin^2(\frac{1}{2}\theta)]^{-1}, \quad (4)$$

separated from E_0 by slightly less than the deuteron binding energy. The inelastic scattering continuum corresponds to values of E_e' less than the end-point energy E_0 (the threshold for deuteron breakup with respect to p). Finally the large inelastic peak corresponding mainly to scattering in which the entire momentum transfer q is absorbed by a single nucleon occurs at a final electron energy for which $p^2 \approx \frac{1}{4}q^2$,

$$(E_e')_{peak} = (E_e - \epsilon)[1 + (2E_e/m) \sin^2(\frac{1}{2}\theta)]^{-1}. \quad (5)$$

The calculation of $d^2\sigma/(d\Omega_e dE_e')$ including the effects of the strong interactions present between the outgoing nucleons was considered in Sec. I of (I).⁹ The electron was treated as an ultrarelativistic particle, and its interaction with the two-nucleon system was calculated in the first Born approximation. However, it was noted that the standard nonrelativistic Hamiltonian used by

Jankus⁸ to describe the interaction of the nucleons with the field of the scattered electron contains only terms through $O(m^{-1})$ in an expansion of the relativistic interaction in inverse powers of the nucleon mass (powers of the nucleon velocity). Since the magnetic moment terms which dominate in the cross section at large momentum transfers appear there multiplied by m^{-2} , it is necessary for consistency to retain in the Hamiltonian terms of this order. The necessary modifications of the interaction Hamiltonian are easily derived by using wave functions of the Breit type to describe the initial and final states of the two-nucleon system, and approximating the current operator for a bound nucleon by the free nucleon operator.⁹ Form factors for the nucleons appear naturally in this procedure. An alternative derivation of an effective interaction to be used with nonrelativistic wave functions for the nucleons is given in Sec. IV of the present paper. Contributions to the cross section involving the D -state component of the deuteron wave function were neglected in the main body of (I), but were considered separately in an Appendix. The nonrelativistic deuteron wave function was therefore chosen to correspond to a pure 3S_1 state,

$$\psi_d^m = (4\pi)^{-\frac{1}{2}} r^{-1} u(r) \chi_1^m(s_1, s_2), \quad (6)$$

with $u(r)$ satisfying the normalization condition

$$\int_0^\infty u^2(r) dr = 1. \quad (7)$$

The final state of the neutron-proton system was described by wave functions distorted by the two-nucleon interactions, but coupling between states of the same total angular momentum J and the same parity, but having different orbital angular momenta L , was neglected. Thus the wave functions for a final state were expressed in terms of the usual orthonormal angular momentum eigenfunctions $\mathcal{Y}_{JMLS}(\hat{r}, s_1, s_2)$ for definite J , L , and spin angular momentum S as

$$\psi_{JMLS} = (\mathbf{pr})^{-1} F_{JLS}(\mathbf{pr}) \mathcal{Y}_{JMLS}(\hat{r}, s_1, s_2), \quad (8)$$

with the radial wave functions $F_{JLS}(\mathbf{pr})$ subject to the asymptotic condition

$$F_{JLS}(\mathbf{pr}) \rightarrow \sin(\mathbf{pr} - \frac{1}{2}L\pi + \delta_{JLS}), \quad \mathbf{pr} \gg L. \quad (9)$$

A straightforward calculation using the foregoing wave functions and the semi-relativistic interaction Hamiltonian led to the result for the inelastic electron scattering cross-section $d^2\sigma/(d\Omega_e dE_e')$ given in Eqs. (7) and (10) of (I):

$$d^2\sigma/(d\Omega_e dE_e') = \sigma_{\text{Mott}} \pi^{-1} m p (m/E) I(\theta, E_e'), \quad (10)$$

where σ_{Mott} is the Mott cross section for the scattering

of a relativistic electron by an external Coulomb field,¹¹

$$\sigma_{\text{Mott}} = \frac{1}{4} \alpha^2 E_e^{-2} \sin^{-4}(\frac{1}{2}\theta) \cos^2(\frac{1}{2}\theta). \quad (11)$$

We have here neglected the electron mass energy relative to E_e and E_e' , and have used units with $\hbar=c=1$ and $\alpha=1/137$. E is the energy of either of the outgoing nucleons in their center-of-mass system. The angular distribution function $I(\theta, E_e')$ is given in the neighborhood of the quasi-elastic peak by

$$\begin{aligned} I(\theta, E_e') = & \frac{1}{3} \sum_{J,L} (2J+1) (K_{J,L,1})^2 \{ [1 - (q/2m)^2] \\ & \times [F_{1p} + (-1)^L F_{1n}]^2 - 2(q/2m)^2 \\ & \times [F_{1p} + (-1)^L F_{1n}] [\kappa_p F_{2p} \\ & + (-1)^L \kappa_n F_{2n}] \} + \frac{1}{3} (q/2m)^2 [2 \tan^2(\frac{1}{2}\theta) + 1] \\ & \times \sum_L \{ \frac{1}{2} [F_{1p} + (-1)^L F_{1n}]^2 + \kappa_p F_{2p} \\ & + (-1)^L \kappa_n F_{2n} \}^2 [(3L+4) (K_{L+1,L,1})^2 \\ & + (2L+1) (K_{L,L,1})^2 + (3L+1) (K_{L-1,L,1})^2] \\ & + [F_{1p} - (-1)^L F_{1n} + \kappa_p F_{2p} - (-1)^L \kappa_n F_{2n}]^2 \\ & \times (2L+1) (K_{L,L,0})^2 \}. \quad (12) \end{aligned}$$

Here κ_p and κ_n are the anomalous parts of the proton and neutron magnetic moments expressed in units of the nuclear magneton. The proton and neutron charge form factors F_{1p} and F_{1n} and the anomalous magnetic moment form factors F_{2p} and F_{2n} are functions of the square of the invariant 4-momentum transfer $q^2 = 4E_e E_e' \sin^2(\frac{1}{2}\theta)$, and are normalized to unity for $q^2=0$, with the exception of F_{1n} , which vanishes at that point. Finally, the radial matrix elements K_{JLS} labeled by the total, orbital, and spin angular momenta of the final state of the neutron-proton system are defined by the relation

$$K_{JLS} = p^{-1} \int_0^\infty F_{JLS}(\mathbf{pr}) j_L(\frac{1}{2}qr) u(r) dr, \quad (13)$$

where $u(r)$ and $F_{JLS}(\mathbf{pr})$ are defined in Eqs. (6) and (8), and $j_L(z)$ is the spherical Bessel function of order L , $j_L(z) = (\pi/2z)^{\frac{1}{2}} J_{L+\frac{1}{2}}(z)$.

The formula for $I(\theta, E_e')$ given in Eq. (12) is too cumbersome to be used for practical calculations, since for the energies and momentum transfers characteristic of the Stanford scattering experiments,⁴ the number of states contributing significantly to the sum is very large. It is therefore more convenient to work with the difference between $I(\theta, E_e')$ and the function $I_0(\theta, E_e')$ which is obtained by neglecting the effects of final state interactions between the nucleons. In the absence of such interactions, the radial wave-functions $F_{JLS}(\mathbf{pr})/\mathbf{pr}$ reduce to the spherical Bessel functions $j_L(\mathbf{pr})$. The matrix elements defined in Eq. (13) are then independent of J and S , and $K_{JLS} \rightarrow K_L$ for all J and S , where

$$K_L = \int_0^\infty j_L(\mathbf{pr}) j_L(\frac{1}{2}qr) u(r) r dr. \quad (14)$$

The expression for $I(\theta, E_e')$ with K_L substituted for

¹¹ W. Heitler, *Quantum Theory of Radiation* (Clarendon Press, Oxford, 1954), third edition, p. 241.

K_{JLS} can be written in the form

$$I_0(\theta, E_e') = M(p, q) \{ F_{1p}^2 + F_{1n}^2 + (q/2m)^2 \\ \times [\kappa_p^2 F_{2p}^2 + \kappa_n^2 F_{2n}^2] + 2(q/2m)^2 \tan^2(\frac{1}{2}\theta) \\ \times [(F_{1p} + \kappa_p F_{2p})^2 + (F_{1n} + \kappa_n F_{2n})^2] \} \\ + N(p, q) \{ \frac{1}{3}(q/m)^2 \tan^2(\frac{1}{2}\theta) \\ \times [(F_{1p} + \kappa_p F_{2p})(F_{1n} + \kappa_n F_{2n})] \\ + [2 - \frac{1}{3}(q/m)^2] F_{1p} F_{1n} - \frac{1}{3}(q/m)^2 \\ \times [\kappa_n F_{1p} F_{2n} + \kappa_p F_{2p} F_{1n}] \\ + \frac{1}{6}(q/m)^2 \kappa_p \kappa_n F_{2p} F_{2n} \}, \quad (15.1)$$

where

$$M(p, q) = \sum_L (2L+1) K_L^2 = \frac{1}{2} \int_0^\pi F^2(\theta) d(\cos\theta), \quad (15.2)$$

$$N(p, q) = \sum_L (2L+1) (-1)^L K_L^2 \\ = \frac{1}{2} \int_0^\pi F(\theta) F(\pi - \theta) d(\cos\theta), \quad (15.3)$$

and

$$F(\theta) = \sum_L (2L+1) P_L(\cos\theta) K_L \\ = \int_0^\infty j_0[\frac{1}{4}q^2 + p^2 - pq \cos\theta]^{\frac{1}{2}} u(r) r dr. \quad (15.4)$$

Introducing next a quantity Δ_{JLS} ,

$$\Delta_{JLS} = (K_{JLS})^2 - (K_L)^2, \quad (16)$$

and a set of coefficients C_{JLS} , we write $I(\theta, E_e')$ in the useful form

$$I(\theta, E_e') = I_0(\theta, E_e') + \sum_{JLS} C_{JLS} \Delta_{JLS}. \quad (17)$$

The coefficients C_{JLS} are as follows:

$$C_{L+1, L, 1} = (2L+3) [a_1 + (-1)^L a_2] \\ + (3L+4) [a_3 + (-1)^L a_4], \\ C_{L, L, 1} = (2L+1) [a_1 + a_3 + (-1)^L (a_2 + a_4)], \\ C_{L-1, L, 1} = (2L-1) [a_1 + (-1)^L a_2] \\ + (3L-1) [a_3 + (-1)^L a_4], \\ C_{L, L, 0} = (4L+2) [a_3 - (-1)^L a_4],$$

where

$$a_1 = \frac{1}{3} [1 - (q/2m)^2] [F_{1p}^2 + F_{1n}^2] \\ - \frac{2}{3} (q/2m)^2 [\kappa_p F_{1p} F_{2p} + \kappa_n F_{1n} F_{2n}], \\ a_2 = \frac{2}{3} [1 - (q/2m)^2] F_{1n} F_{1p} - \frac{2}{3} (q/2m)^2 \\ \times [\kappa_p F_{1n} F_{2p} + \kappa_n F_{2n} F_{1p}], \\ a_3 = \frac{1}{6} (q/2m)^2 [2 \tan^2(\frac{1}{2}\theta) + 1] [(F_{1p} + \kappa_p F_{2p})^2 \\ + (F_{1n} + \kappa_n F_{2n})^2], \\ a_4 = \frac{1}{3} (q/2m)^2 [2 \tan^2(\frac{1}{2}\theta) + 1] (F_{1p} + \kappa_p F_{2p}) \\ \times (F_{1n} + \kappa_n F_{2n}). \quad (19)$$

The C_{JLS} are precisely the coefficients with which each possible final state of the neutron-proton system contributes to the cross section; we can obviously write $I(\theta, E_e')$ in the form

$$I(\theta, E_e') = \sum_{JLS} C_{JLS} (K_{JLS})^2, \quad (12')$$

which is useful in cases in which only a few matrix elements differ from zero (see Sec. III).

In the following sections we will be concerned with calculations of $I(\theta, E_e')$ and of the difference between $I(\theta, E_e')$ and $I_0(\theta, E_e')$ caused by the presence of significant interactions between the outgoing nucleons. It will be necessary to consider only a limited number of final states for the neutron-proton system, since the quantities Δ_{JLS} vanish unless the radial wave-function $F_{JLS}(pr)/pr$ differs appreciably from $j_L(pr)$; this will only occur if the corresponding neutron-proton scattering phase shift δ_{JLS} is large.

II. EFFECTS OF FINAL-STATE INTERACTIONS AT THE PEAK IN $d^2\sigma/(d\Omega_e dE_e')$

The main difficulty in calculating the effects of interactions between the outgoing nucleons on $d^2\sigma/(d\Omega_e dE_e')$ is in the evaluation of the radial matrix elements K_{JLS} , Eq. (13). This requires knowledge of both the deuteron wave function and the free state wave functions for given J, L, S and nucleon center-of-mass momentum p . While calculations using numerical wave functions computed from one of the phenomenological neutron-proton potential models¹²⁻¹⁴ would appear to be desirable, it was felt that the fundamental features of the corrections could be understood using a very simple model. The 3S_1 component of the deuteron wave function was represented by a Hulthén wave function matched to the observed low-energy parameters of the neutron-proton system. In treating the wave-functions $F_{JLS}(pr)$ for the final states, it was noted that outside the range of the internucleon force, $F_{JLS}(pr)$ has the form

$$F_{JLS}(pr) \rightarrow \cos\delta_{JLS} F_L(pr) + \sin\delta_{JLS} G_L(pr), \quad (20)$$

where δ_{JLS} is the asymptotic phase shift appearing in Eq. (9), and $F_L(pr)$ and $G_L(pr)$ are the regular and irregular solutions of the Schrödinger equation in the absence of nuclear forces, $F_L(x) = (\pi x/2)^{\frac{1}{2}} J_{L+\frac{1}{2}}(x)$, $G_L(x) = (-1)^L (\pi x/2)^{\frac{1}{2}} J_{-L-\frac{1}{2}}(x)$. The phase shifts δ_{JLS} are known with reasonable certainty in the range 0-300 Mev from the results of recent analyses of the nucleon-nucleon scattering experiments.¹³⁻¹⁶ For the electron energies and scattering angles typical of the Stanford electron-deuteron scattering experiments, the

¹² J. L. Gammel and R. M. Thaler, Phys. Rev. **107**, 291, 1337 (1957).

¹³ P. S. Signell and R. E. Marshak, Phys. Rev. **106**, 832 (1957); **109**, 1229 (1958). P. S. Signell, R. Zinn, and R. E. Marshak, Phys. Rev. Letters, **1**, 416 (1958).

¹⁴ R. A. Bryan, Bull. Am. Phys. Soc. **5**, 35 (1960), and Nuovo cimento (to be published). The author is indebted to Dr. Bryan for supplying the phase shifts listed in Table I, and for information on the corresponding fits to the neutron-proton scattering data.

¹⁵ G. Breit, M. H. Hull, Jr., K. E. Lassila, and K. D. Pyatt, Jr., Phys. Rev. **120**, 2227 (1960). M. H. Hull, Jr., K. E. Lassila, H. M. Ruppel, F. A. McDonald, and G. Breit, *ibid.* **122**, 1606 (1961). The author would like to thank Professor Breit for pre-publication information concerning these analyses of the proton-proton and neutron-proton scattering data below 350 Mev.

¹⁶ M. H. MacGregor, M. J. Moravcsik, and H. P. Stapp, Phys. Rev. **116**, 1248 (1959).

TABLE I. The phase shifts (in degrees) of the Bryan-Signell-Marshak fit to the neutron-proton scattering data at laboratory energies for the incident nucleon of 150 and 240 Mev. The 3S_1 , 3D_1 , 1P_1 , and 1F_3 phase shifts are those calculated by Signell and Marshak^a; the remainder are those given by Bryan.^b The combined set gives a reasonably good fit to the relevant scattering data.^b The center-of-mass wave numbers are $p=1.34 \text{ f}^{-1}$ for $E=150 \text{ Mev}$, $p=1.7 \text{ f}^{-1}$ for $E=240 \text{ Mev}$. The coupling between states of the same J and $L=J\pm 1$ represented by the coupling parameters ϵ_J was omitted in the calculations described in Sec. II.

$E(\text{Mev})$	L	$\delta_{L+1, L, 1}$	$\delta_{L, L, 1}$	$\delta_{L-1, L, 1}$	$\delta_{L, L, 0}$	ϵ_J
150	0	22.6	18.7	...
	1	13.7	-16.8	4.7	-22.1	3.9
	2	9.4	25.4	-23.1	5.2	-13.5
	3	1.2	-2.0	0.3	-3.9	26.5
240	0	7.8	5.2	...
	1	16.6	-23.1	-4.1	-27.3	2.8
	2	14.9	33.2	-32.0	9.2	-11.0
	3	2.6	-3.0	0.7	-5.5	19.5

^a See reference 13.

^b See reference 14.

values of the momentum p of the nucleons in their center-of-mass system are in fact equivalent to those obtained in neutron-proton scattering experiments in this energy range. For example, the quasi-elastic peak occurs for incident electrons of 500 Mev scattered through 135° at an energy $E_e'=261 \text{ Mev}$, corresponding to a value of p of 1.69 f^{-1} ; this relative momentum for the nucleons is attained in a neutron-proton scattering experiment for an energy of 237 Mev for the incident nucleon. Similarly, for $E_e=500 \text{ Mev}$, $\theta=75^\circ$, the quasi-elastic peak is at 357 Mev, $p=1.30 \text{ f}^{-1}$, and the equivalent scattering energy is 141 Mev. The n - p phase shifts at 150 and 240 Mev given by the Bryan-Signell-Marshak fit^{13,14} to the nucleon-nucleon scattering data are listed in Table I. For both energies, a number of the phase shifts for the states with $L\leq 2$ are quite large. The corresponding wave-functions $F_{JLS}(pr)$ therefore differ significantly from the $F_L(pr)$, and it may in general be expected that the matrix elements K_{JLS} will be poorly approximated by the matrix elements K_L calculated with the neglect of interactions between the outgoing nucleons.¹⁷

¹⁷ The fact that for those values of q of the most interest, the center-of-mass energy of the emerging nucleons lies in a region in which the scattering phase shifts are known to be large is in itself sufficient to cast considerable doubt upon the validity either of neglecting entirely the effects of final-state interactions, or of treating these effects in Born approximation. The argument may be made somewhat more precise as follows. Contributions to the cross section from states with high orbital angular momenta are small, the largest value of L which can appear being given roughly by the requirement that the classical turning point in the scattering process lie inside the deuteron, $L_{\max}\approx p/\alpha$, where α^{-1} is the deuteron "radius." Similarly, the largest value of L for which there can be important effects of final-state interactions is determined by the requirement that the classical turning point lie within the range of the neutron-proton interaction, $L_{\text{int}}\approx p/\mu$. Thus, the ratio of the number of final states in which interactions are strong to the total number which contribute significantly to the cross section $d^2\sigma/(d\Omega dE_e')$ is roughly $\alpha/\mu\approx\frac{1}{3}$, independent of p and q . Detailed calculations give a slightly larger fraction, on the order of 0.4-0.5. Thus, while the large separation of the nucleons in the deuteron reduces the over-all effect of final state interactions, the reduction is only by a factor of 2-3, and significant corrections to

Investigations by Bryan¹⁴ using a semiphenomenological potential model of the nucleon-nucleon interaction indicate that at 300 Mev, the greater part of the phase shift for states with $L=0, 1$ and 2 originates in the region of internucleon separations 0-1, 0.4-1.4, and 0.8-1.8 f, respectively. For the lower scattering energies of interest here, these regions will be shifted to larger values of r , but it is likely that the wave functions with $L\leq 2$ will in any case attain the asymptotic form given in Eq. (20) for $r\gtrsim r_0=2 \text{ f}$. Moreover, the region $r\geq 2.0 \text{ f}$ contributes 28%, 54%, and 87% of the matrix elements K_0, K_1 , and K_2 for $p=1.3 \text{ f}^{-1}$, and 35%, 37%, and 68% of the same matrix elements for $p=1.7 \text{ f}^{-1}$. Considering the magnitude of the phase shifts δ_{JLS} for $L\leq 2$, it is evident that the contributions of this exterior region will be changed significantly if $F_L(pr)$ is replaced by the correct asymptotic form of $F_{JLS}(pr)$, Eq. (20). The exact wave-functions $F_{JLS}(pr)$ which enter the definition of K_{JLS} will, of course, differ appreciably from the free-particle wave functions $F_L(pr)$ for $r<r_0$ as well. In this region our knowledge of the wave functions is quite limited unless a specific potential model is used, but it would appear to be a reasonable approximation to replace the correct wave functions by those corresponding to a constant potential,

$$F_{JLS}(pr) \rightarrow \gamma_{JLS} F_L(\lambda_{JLS} r), \quad (21)$$

requiring, however, that γ_{JLS} and λ_{JLS} be so chosen that this interior wave function join properly at the radius r_0 to the external wave function of Eq. (20) with the experimentally known phase shift δ_{JLS} . This requirement is expressed in the well-known equations

$$(\lambda/p)F_L'(\lambda r_0)/F_L(\lambda r_0) = [F_L'(pr_0) + \tan\delta G_L'(pr_0)] \times [F_L(pr_0) + \tan\delta G_L(pr_0)]^{-1}, \quad (22)$$

and

$$\gamma = [\cos\delta F_L(pr_0) + \sin\delta G_L(pr_0)] [F_L(\lambda r_0)]^{-1}, \quad (23)$$

where $F_L'(x)$ and $G_L'(x)$ are the derivatives of F_L and G_L , and we have for simplicity suppressed the subscripts on γ, λ , and δ . Since the phase shifts are known, we are in effect matching a square well potential to δ_{JLS} and calculating the associated wave function; this "equivalent square well potential" will in general vary with J, L , and S , and with the momentum p , and is not to be regarded as physically significant.

Some justification for the foregoing model may be found by observing that the matrix element K_{JLS} involves a factor $F_L(\frac{1}{2}qr)/(\frac{1}{2}qr)$ which vanishes for $L>0$ as $(\frac{1}{2}qr)^L/(2L+1)!!$ for $r\rightarrow 0$. Since $u(r)$ and the wave-

the cross section may be present. We remark also that the treatment of final-state interactions given in reference 8 uses a central potential to describe the interactions, neglecting entirely the very strong noncentral forces which lead to the large variations in sign and magnitude of the phase shifts listed in Table I. It should also be noted that the apparent smallness of the effects of final-state interactions near the threshold for the dissociation of the deuteron,¹⁰ $p\approx 0$, is irrelevant to discussion of such effects at the quasi-elastic peak, $p\approx\frac{1}{2}q$; some confusion on this point has existed in the past. The effects near threshold are discussed in detail in Sec. III.

functions $F_{JLS}(pr)$ for $L > 0$ also vanish for $r \rightarrow 0$, the integrand in Eq. (13) is weighted toward large values of r . This may be seen in Fig. 1, which shows the integrand obtained for $L=1$, $p=\frac{1}{2}q=1.3 \text{ f}^{-1}$ and $\delta=+21^\circ$, 0° , and -22° using the foregoing approximation for the final-state wave function and a Hulthén model for the deuteron ground-state wave function. The integrand in each case has its first maximum at a value of r very close to the matching radius r_0 , taken here as 2.0 f. However, for r near r_0 , the possible variation in the true interior wave function from the form assumed in Eq. (21) is small for reasonable potentials, being limited by the necessity that the wave function join properly at $r=r_0$ to its known asymptotic form. Since the asymptotic phase shifts are known, the major uncertainty is probably in the proper choice of r_0 . It is furthermore evident from Fig. 1 that the approximations which have been made should be somewhat better for small than for large values of p ($\frac{1}{2}q=p$ at the quasi-elastic peak), and for negative than for positive phase shifts, either a small p or a negative phase shift tending to reduce the importance of the interior as compared to the exterior region. Similar (and stronger) arguments apply to the states with $L=2$. For the states with $L=0$, the argument is less convincing, but it is fortunately not necessary to know very accurately the changes in the matrix elements associated with final state interactions, the S states contributing only 10% and 5% of the peak cross section at $p=1.3 \text{ f}^{-1}$ and $p=1.7 \text{ f}^{-1}$ compared to 22% and 18% for the P states, and 16% and 11% for the D states.

The matrix elements K_{JLS} were calculated using the final-state wave functions of Eqs. (20) and (21), and assuming a Hulthén model for the deuteron wave function,¹⁸

$$u(r) = N[e^{-\alpha r} - e^{-\beta r}]. \quad (24)$$

Noting that $j_L(\frac{1}{2}qr) = (\frac{1}{2}qr)^{-1}F_L(\frac{1}{2}qr)$, we have from Eq. (13)

$$\begin{aligned} K_{JLS}(p,q) &= \frac{2}{pq} \int_0^\infty F_{JLS}(pr) F_L(\frac{1}{2}qr) u(r) r^{-1} dr \\ &= \frac{2}{pq} \int_0^\infty [\cos \delta_{JLS} F_L(pr) \\ &\quad + \sin \delta_{JLS} G_L(pr)] F_L(\frac{1}{2}qr) u(r) r^{-1} dr \\ &\quad + \frac{2}{pq} \int_0^{r_0} [\gamma_{JLS} F_L(\lambda_{JLS} r) \\ &\quad - \cos \delta_{JLS} F_L(pr) - \sin \delta_{JLS} G_L(pr)] \\ &\quad \times F_L(\frac{1}{2}qr) u(r) r^{-1} dr. \end{aligned} \quad (25)$$

The integral over the finite segment $0 \leq r \leq r_0$ is most simply evaluated numerically, while that over the infi-

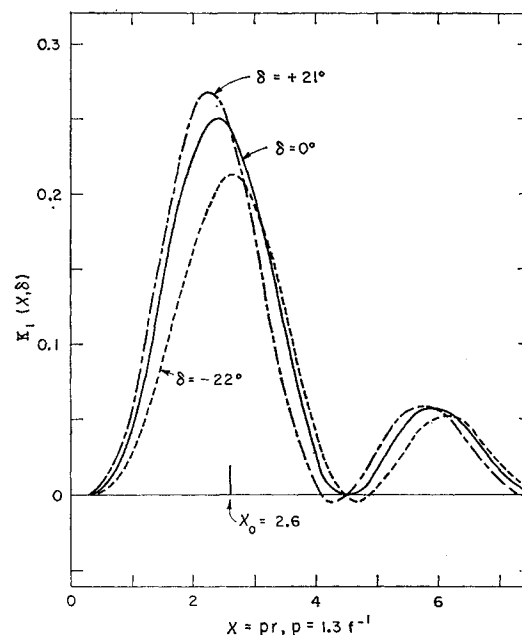


FIG. 1. The integrand for the matrix elements $K_{JLS}(p,q)$ for $p=\frac{1}{2}q=1.3 \text{ f}^{-1}$ as computed using the approximate initial and final state wave function given in Eqs. (20), (21), and (24), with $K_{JLS}(p,q) = (4N/q^2) \int_0^\infty K_1(x, \delta_{JLS}) dx$. The interior and exterior wave functions were matched at a radius $r_0=2.0 \text{ f}$, $x_0=2.6$. The matrix element for $\delta=-22^\circ$ is 13% smaller than that computed in the absence of final-state P -wave interactions between the nucleons [$\delta=0^\circ$], while that for $\delta=+21^\circ$ is 0.5% larger. Complete curves of the fractional change in the matrix elements versus δ are given in Figs. 2 and 3.

nite interval $0 \leq r < \infty$ may easily be expressed in closed form when $u(r)$ consists of a sum of exponentials as in Eq. (24). The necessary relations, specialized to the condition $\frac{1}{2}q=p$ corresponding to the quasi-elastic peak in the cross-section $d^2\sigma/(d\Omega dE_e')$, are

$$\int_0^\infty [F_L(x)]^2 e^{-ax} x^{-1} dx = \frac{1}{2} Q_L(1 + \frac{1}{2}a^2), \quad (26)$$

and

$$\begin{aligned} \int_0^\infty F_L(x) G_L(x) e^{-ax} x^{-1} dx \\ = \frac{1}{2} (-1)^L \int_0^{\pi/2} \frac{\cos(2L+1)\phi d\phi}{[(a^2/4) + \cos^2\phi]^{\frac{1}{2}}}. \end{aligned} \quad (27)$$

Here Q_L is the Legendre function of the second kind. The remaining integral in Eq. (27) is easily reduced to a collection of inverse tangents and polynomials. The resulting expressions for the infinite integrals in Eq. (25) are rather lengthy, but are straightforward to derive. We note also that the matrix element K_L , Eq. (14), which enters the definition of Δ_{JLS} , Eq. (16), is given for arbitrary p, q by:

$$K_L(p,q) = (N/pq) [Q_L(x) - Q_L(y)], \quad (28)$$

¹⁸ L. Hulthén and M. Sugawara, *Handbuch der Physik*, edited by S. Flügge, (Springer-Verlag, Berlin, 1957), Vol. 39.

where [compare Eqs. (83)]

$$x = (\alpha^2 + p^2 + \frac{1}{4}q^2)/pq,$$

$$y = (\beta^2 + p^2 + \frac{1}{4}q^2)/pq.$$

Finally, one obtains for the functions $M(p, q)$ and $N(p, q)$ defined in Eqs. (15)

$$M(p, q) = [N^2/(pq)^2] \left\{ [x^2 - 1]^{-1} + [y^2 - 1]^{-1} - \frac{1}{y - x} \ln \left[\frac{x+1}{x-1} \frac{y-1}{y+1} \right] \right\}, \quad (29)$$

and

$$N(p, q) = \frac{1}{2} \frac{N^2}{(pq)^2} \left\{ \frac{1}{x} \ln \frac{x+1}{x-1} + \frac{1}{y} \ln \frac{y+1}{y-1} - \frac{2}{x+y} \ln \left[\frac{x+1}{x-1} \frac{y+1}{y-1} \right] \right\}. \quad (30)$$

Those terms in the function $I_0(\theta, E_e')$, Eq. (15.1), which involve $N(p, q)$ arise from interference between electrons scattered off the proton and those scattered off the neutron. These interference effects are entirely negligible at the peak of the inelastic electron spectrum, and will be omitted. As shown in the Appendix, the function $M(p, q)$ may be approximated at the peak by

$$M(p, q) = \frac{1}{4} (N^2/p^2) [\alpha^{-2} + \beta^{-2} - 2(\beta^2 - \alpha^2)^{-1} \ln(\beta^2/\alpha^2)] \\ = (2.962 \times 10^{-13} \text{ cm}) p^{-2}, \quad \frac{1}{2}q = p. \quad (31)$$

The foregoing expression for $M(p, 2p)$ is accurate to within 1.4% for $p = \frac{1}{2}q = 1.0 \text{ f}^{-1}$, and the errors decrease as p^{-6} for larger values of p .

Numerical results for the change in the peak value of the cross-section $d^2\sigma/(d\Omega_d dE_e')$ caused by interactions between the outgoing nucleons were obtained as follows. The matrix elements K_{JLS} and K_L and the quantities Δ_{JLS} which enter in Eq. (17) for the corrected cross section were calculated using the approximate wave functions given in Eqs. (20), (21), and (24). The phase shifts δ_{JLS} were taken from the Bryan-Signell-Marshak fit to the nucleon-nucleon scattering data below 300 Mev [see Table I],^{13,14} but the coupling between states of the same J and S with $L = J \pm 1$ was ignored. This should introduce little error in the results. Lacking at those values of p which were of interest here detailed information about the radius r_0 of which the wavefunction $F_{JLS}(pr)$ attains substantially its asymptotic form, we have used in our calculations the value $r_0 = 2.0 \text{ f}$. This is undoubtedly too large for the S states, but appears to be a reasonable value for the P states and probably the D states as well. As a practical matter, it was simplest in using the matching condition of Eq. (22) to assume a set of values for the parameter λ and to calculate the corresponding values of δ_{JLS} and K_{JLS} . The value of the matrix element corresponding to the experimentally determined phase shift was then obtained graphically. The quantity R_L which gives the fractional change in the matrix elements of order L caused by final-state interactions,

$$R_L = [K_{JLS} - K_L]/K_L,$$

is plotted in Fig. 2 for $p = 1.3 \text{ f}^{-1}$ and $L = 0, 1, 2$; the same quantities are shown in Fig. 3 for $p = 1.7 \text{ f}^{-1}$. It is seen that the changes in the matrix element associated with phase shifts on the order of those in Table I are

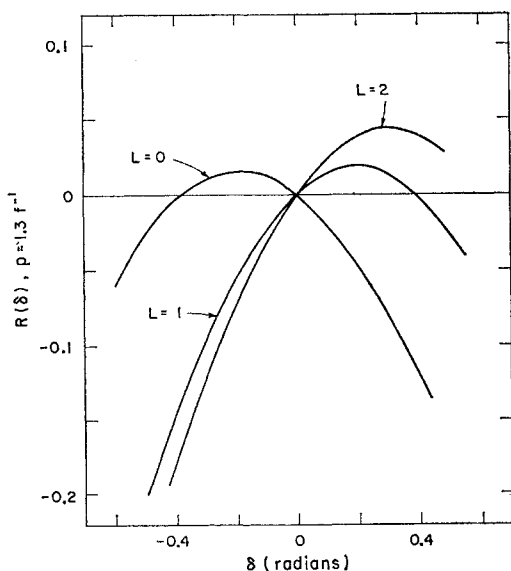


FIG. 2. The fractional change $R(\delta)$ in the matrix elements $K_{JLS}(p, q)$ relative to the matrix elements $K_L(p, q)$ defined for vanishing final-state interactions, calculated for $p = \frac{1}{2}q = 1.3 \text{ f}^{-1}$ using the approximation given in Eq. (25).

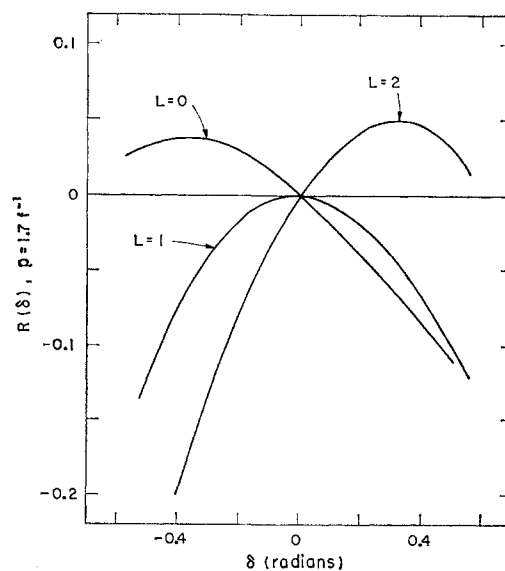


FIG. 3. The fractional change $R(\delta)$ in the matrix elements $K_{JLS}(p, q)$ relative to the matrix elements $K_L(p, q)$ defined for vanishing final-state interactions, calculated for $p = \frac{1}{2}q = 1.7 \text{ f}^{-1}$ using the approximation given in Eq. (25).

in some cases remarkably large. In Tables II and III we give the values of the quantities $D_{JLS} = \Delta_{JLS}/(K_L)^2$ and $c_{JLS} = C_{JLS}K_L^2/I_0(\theta, E_e')$ for the parameters corresponding to the quasi-elastic peak for momentum transfers $q=2.6, 3.4 \text{ f}^{-1}$, and scattering angles $\theta=75^\circ, 135^\circ$. The numbers D_{JLS} are the fractional changes in the squares of the matrix elements associated with final state interactions, while the coefficients c_{JLS} are the fractional weights of each state in the cross section without final-state interactions. The over-all change in the peak cross section, $[I(\theta, E_e') - I_0(\theta, E_e')]/I_0(\theta, E_e')$, is obtained by multiplying the numbers in the same locations in the two tables and summing. In calculating $I_0(\theta, E_e')$ and the coefficients c_{JLS} , we have assumed that $F_{1p} \approx F_{2p} \approx F_{2n}$, and that $F_{1n} \approx 0$, in accord with the results of the Stanford experiments.⁴ Our results are insensitive to small deviations from these conditions.

The dependence of $R_L(\delta)$ on δ shown in Figs. 2 and 3 is easily understood. As may be seen from Fig. 1, the value of the integral giving the matrix elements K_{JLS} is largely determined by the first peak in the integrand. It is convenient to consider separately the dependence of this peak on the deuteron wave-function $u(r)$ and on the function $F_{JLS}(pr)F_L(\frac{1}{2}qr)/(\frac{1}{2}qr)$. We shall take $p=\frac{1}{2}q$ and $x=\frac{1}{2}qr$. If interactions between the outgoing nucleons are neglected, $F_{JLS}(x)$ is replaced by $F_L(x)$, and the second factor in the integrand becomes simply $x^{-1}[F_L(x)]^2$. This function has its first maximum at $x=1.17, 2.46$, and 3.64 for $L=0, 1$, and 2 , while, for $p=\frac{1}{2}q=1.3 \text{ f}^{-1}$, $u(r)$ reaches its maximum value at $x=1.98$. Thus a small positive phase shift in $F_{JLS}(x)$, by shifting the first maximum in $x^{-1}F_{JLS}(x)F_L(x)$ away from that in $x^{-1}[F_L(x)]^2$ and in the direction of smaller x will bring the peaks in the two factors of the integrand more nearly into coincidence for $L=1$ and 2 , and will decrease the overlap of the peaks for $L=0$. Consequently, for small positive phase shifts, K_{JLS} will be larger than K_L , hence, $R_L > 0$, for $L=1$ and 2 , while for $L=0$, K_{JLS} will be smaller than K_0 , and $R_0 < 0$. We remark however, that the function $x^{-1}F_{JLS}(x)F_L(x)$ assumes negative as well as positive values for non-vanishing phase shifts δ_{JLS} . In fact, for sufficiently large positive $L=1$ and $L=2$ phase shifts, the increase in the integrands in the region of the first peak will be offset

TABLE II. The quantities $D_{JLS} = \Delta_{JLS}/(K_L)^2$ which give the fractional changes in the radial matrix elements K_{JLS} associated with the effects of interactions between the outgoing nucleons. The matrix elements are calculated for parameters $\frac{1}{2}q=p$ corresponding to the peak in the spectrum of inelastically scattered electrons.

$p \text{ (f}^{-1}\text{)}$	L	$D_{L+1, L, 1}$	$D_{L, L, 1}$	$D_{L-1, L, 1}$	$D_{L, L, 0}$
1.3	0	-0.219	-0.174
	1	0.036	-0.176	0.024	-0.252
	2	0.071	0.073	-0.328	-0.044
1.7	0	-0.053	-0.037
	1	-0.075	-0.144	-0.004	-0.212
	2	0.096	0.016	-0.513	0.077

TABLE III. Representative values of the coefficients $c_{JLS} = C_{JLS}K_L^2/I_0(\theta, E_e')$ giving the fractional contribution of the final state of the neutron-proton system labelled by angular momenta J, L, S to the peak cross section in the absence of final-state interactions between the nucleons. The coefficients were calculated in the approximation $F_{1n}=0, F_{2n} \approx F_{1p} \approx F_{2p}$.

$q \text{ (f}^{-1}\text{)}$	θ	L	$c_{L+1, L, 1}$	$c_{L, L, 1}$	$c_{L-1, L, 1}$	$c_{L, L, 0}$
2.6	75°	0	0.046	0.054
		1	0.120	0.055	0.034	0.004
		2	0.034	0.024	0.015	0.085
2.6	135°	0	0.015	0.069
		1	0.141	0.061	0.040	0.005
		2	0.011	0.007	0.005	0.108
3.4	75°	0	0.020	0.039
		1	0.089	0.038	0.026	0.003
		2	0.020	0.014	0.009	0.083
3.4	135°	0	0.006	0.043
		1	0.100	0.043	0.029	0.003
		2	0.006	0.004	0.003	0.092

by decreased and negative contributions from other ranges of x , and K_{JLS} will become smaller than K_L . For negative phase shifts in the $L=1$ and $L=2$ states, the situation is reversed, and K_{JLS} decreases rapidly with increasing $|\delta_{JLS}|$ as a consequence both of diminished overlap of the peaks of the two factors, and of the presence of the oscillating components in the integrand. The integrands for $L=1, p=\frac{1}{2}q=1.3 \text{ f}^{-1}$, and $\delta=+22^\circ, 0^\circ$, and -21° are plotted in Fig. 1, and the effects of the phase shifts may easily be seen. The roles played by positive and negative phase shifts in the foregoing are interchanged for the $L=0$ states, but the analysis is otherwise unchanged. The expected behavior of $R_L(\delta)$ clearly reflected by the curves of Fig. 2. The situation is similar for $p=\frac{1}{2}q=1.7 \text{ f}^{-1}$, and will not be discussed in detail. However, it is interesting to note that the maximum in $u(r)$ now corresponds to $x=2.58$, a point very close to the first maximum in $x^{-1}[F_L(x)]^2$ at $x=2.46$. As would be expected, $R_1(\delta)$ is nearly symmetric about $\delta=0$.

The effects of final-state interaction on the peak value of $d^2\sigma/(d\Omega_e dE_e')$ are summarized in Table IV for $q=2.6, 3.4 \text{ f}^{-1}$, and various scattering angles. In every case, the peak cross section is decreased, the correction varying only slightly with θ . These results are based on the phase shifts given by the Bryan-Signell-Marshak fit to the

TABLE IV. Corrections to the function $I(\theta, E_e')$ at the quasi-elastic peak resulting from interactions between the outgoing neutron and proton.

$q \text{ (f}^{-1}\text{)}$	θ	$\Delta I/I$
2.6	45°	-0.0245
	75°	-0.0221
	105°	-0.0191
	135°	-0.0165
3.4	45°	-0.0120
	75°	-0.0113
	105°	-0.0106
	135°	-0.0101

nucleon-nucleon scattering data at 150 and 240 Mev.^{13,14} A separate calculation for $q=2.6 \text{ f}^{-1}$ and $\theta=75^\circ$ using the Gammel-Thaler phase shifts¹² led to a 1.4% decrease in the peak cross section instead of the 2.2% decrease listed in Table IV. The difference in the results for the two fits is associated mainly with differences in the 1S_0 , 1D_2 , 3S_1 , 3D_1 , and 3D_3 phase shifts. Breit *et al.*¹⁵ have remarked that neither value of the 1D_2 phase shift agrees well with that determined from their complete phase shift analysis of the proton-proton scattering data between 10 Mev and 345 Mev and that the Bryan-Signell-Marshak value of the 1S_0 phase shift is definitely too large. The corresponding analysis of the neutron-proton scattering data undertaken by Hull *et al.*¹⁵ indicates that both the Gammel-Thaler and the Bryan-Signell-Marshak values of the 3S_1 phase shift are too small, and the values of the 3D_1 and 3D_3 phase shifts, too large, in magnitude. The "best" value for change in the peak cross section for $p=\frac{1}{2}q=1.3 \text{ f}^{-1}$ and $\theta=75^\circ$ would appear to be about -2% . The corrections at other angles would also be changed somewhat. The discrepancies between the Bryan-Signell-Marshak and the Gammel-Thaler results are illustrative of the uncertainties introduced into the present calculations by errors in the assumed phase shifts. In addition the analyses of Breit *et al.*¹⁵ and Hull *et al.*¹⁵ lead to rather large phase shifts in the F and G states at the higher equivalent scattering energy 240 Mev ($q=3.4 \text{ f}^{-1}$), and it is probable that changes in the associated partial wave matrix elements should be taken into account.

As may be seen from Tables II and III, the unexpected smallness of the final state corrections results primarily from the small weights corresponding to those states with the largest values of Δ_{JLS} [e.g., the 1S_0 , 3S_1 , 1P_1 , 3P_1 , and 3D_1 states for the case $q=2.6 \text{ f}^{-1}$, and the 1P_1 , 3P_1 , and 3D_1 states for $q=3.4 \text{ f}^{-1}$]. The final values are also reduced by factors of roughly 1.5 and 2 for $q=2.6 \text{ f}^{-1}$ and $q=3.4 \text{ f}^{-1}$ by cancellations between positive and negative terms associated with phase shifts of different signs. It is interesting in this context to note that the sign of the over-all correction to the peak cross section is not obvious *a priori*. The weights C_{JLS} with which a given final state contributes to the cross sections, Eq. (12'), are positive [compare (I),⁹ Eq. (7.3)], and we have seen that it is possible either to increase or decrease the matrix elements K_{JLS} by choosing a final state phase shift of the appropriate sign. Thus, with some choice of phase shifts, the peak value of the cross section could be made to increase; the phase shifts determined from nucleon-nucleon scattering experiments lead instead to a small decrease in that quantity. It should, in addition, be remarked that, had we written the cross section as in Eq. (15.1), that is, as a sum of an interference cross section and a "direct" cross section corresponding to scattering off of a single nucleon, the interference cross section would no longer be negligible as was the case in the absence of final state interactions. In fact, for $q=2.6 \text{ f}^{-1}$, and $\theta=75^\circ$ the

interference terms contribute 2.3% of the peak cross section, while for $q=3.4 \text{ f}^{-1}$, and $\theta=135^\circ$ their contribution has increased sharply to 4.9%. The interference terms are positive in each case. Conversely, the contributions to the peak cross section which correspond to the scattering of the electron by a single nucleon are decreased by 4.5% for $q=2.6 \text{ f}^{-1}$, and by 5.8% for $q=3.4 \text{ f}^{-1}$, to give the small over-all corrections quoted above. The foregoing numbers would be changed somewhat by an alteration in the radius r_0 at which the interior and exterior final state wave functions are joined, or, indeed, by changing the entire model for the deuteron and the final-state wave functions. It nevertheless seems probable that the over-all corrections to the peak cross section would remain negative and about the same magnitude as calculated here, our results being in large part determined by the phase shifts derived from experimental studies of neutron-proton scattering. However, more precise calculations using wave functions derived from one of the two-nucleon potentials which fit the high-energy neutron-proton scattering data would be of great interest either in substantiating or modifying the present, largely exploratory, results, and should certainly be undertaken. It is apparent also from the large changes in individual matrix elements associated with the effects of final state interactions, that the results given in (I) for the angular distribution of the emergent nucleons may be significantly altered, but the proposed backward-to-forward ratio method for determining the ratios of the neutron to the proton form factors should remain valid for the reasons noted there.

III. EFFECTS OF FINAL-STATE INTERACTIONS NEAR THE THRESHOLD FOR DEUTERON BREAKUP

For a fixed energy of the incident electron and a given scattering angle, the range of possible final energies for an electron scattered inelastically from the deuteron is bounded above by E_0 , Eq. (13). This energy represents the threshold for the dissociation of the deuteron, the nucleons emerging with vanishing momenta p in their center-of-mass system:

$$p^2 = m(E_0 - E_e') [1 + (E_e'/m) \sin^2(\frac{1}{2}\theta)]. \quad (32)$$

Kendall *et al.*¹⁰ have recently made an extensive study of the cross-section $d^2\sigma/(d\Omega_d dE_e')$ for final electron energies within a few Mev of the threshold. In this region p is small, and the cross section is dominated by the contributions of final S states for the nucleons. Moreover, Jankus⁸ has shown that the S -state matrix elements K_{J0S} are greatly increased by the strong attractive interactions of the nucleons in the final state, causing the cross section to peak sharply near $p=0$. The results of Kendall *et al.*¹⁰ confirm that the peak is present, but the measured cross sections, averaged over a 1-Mev range of energies just below threshold, are generally smaller than predicted by the Jankus theory. This may be seen in Fig. 4.

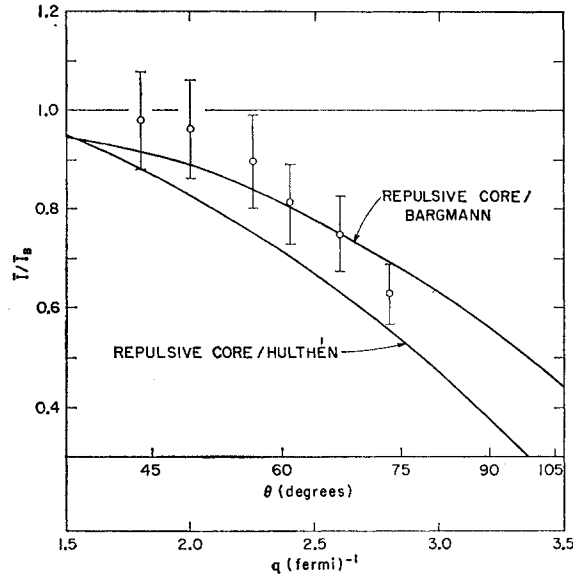


FIG. 4. The ratio of the cross-section $d^2\sigma/(d\Omega_e dE_e')$ integrated over the interval $0 \leq E_0 - E_e' \leq 1$ Mev, to the corresponding quantity calculated from the Jankus theory⁸ using the Bargmann wave functions for the initial and final states of the neutron-proton system. The function $\bar{I}(\theta, E_e, \Delta E)$ describing the integrated cross section is defined in Eq. (50). The parameters are $E_0 = 500$ Mev, $\Delta E = 1$ Mev. The experimental data are those of Kendall *et al.*,¹⁰ while the solid curves are calculated for the models considered in Sec. III.

In both the original calculations of Jankus and subsequent calculations performed at Stanford, the S -state matrix elements K_{J0S} were evaluated using deuteron and final state wave functions corresponding to an Eckart (Bargmann) potential.¹⁹ This choice has the attractive feature that the wave functions are known in closed form. The scattering phase shifts furthermore satisfy exactly the shape-independent effective range expansion. On the other hand, the integral which determines the matrix elements contains a factor $j_0(\frac{1}{2}qr)$ in addition to the product of the wave functions [Eq. (13)]. This factor weights most strongly small values of the internucleon separation r when q is large, and it is precisely for small separations that the Bargmann wave functions may be expected to be least accurate. The facts that the experimental cross sections are smaller than predicted, and that the discrepancy increases with increasing q , suggest strongly that the discrepancy is associated with the neglect of the repulsive core which is present in the two-nucleon interaction.¹²⁻¹⁴ The core was shown by McIntyre *et al.*⁶ to decrease markedly the value of the deuteron form factor F_d observed in elastic electron-deuteron scattering. Since the low-energy S -state scattering wave functions behave for small r roughly like the deuteron wave function, one may similarly expect the core effects to be important in the inelastic scattering near threshold.

The results of the present calculations substantiate this view.

For the remainder of this section, we will be concerned with the calculation of the angular distribution function $I(\theta, E_e')$, Eq. (12), for $E_0 - E_e' \lesssim 1$ Mev. For the 500-Mev incident electron energy used in the bulk of the Stanford experiments,¹⁰ the corresponding values of p lie in the interval $0 \lesssim p \lesssim 0.19$ f⁻¹, and the equivalent neutron-proton scattering energies in the range $0 \leq E_{lab} \lesssim 3.1$ Mev. There is no evidence of any significant interaction of the nucleons in states with $L \geq 1$ for energies in this range. Thus the matrix elements K_{JLS} may be replaced for $L \geq 1$ by the matrix elements K_L for noninteracting particles. The corresponding contributions to $I(\theta, E_e')$ are negligible for the energies of interest, the free wave functions $F_L(pr)$ for small p being strongly suppressed by the angular momentum barrier in the region in which the function $j_0(\frac{1}{2}qr)u(r)$ is large. Retaining only the contributions of the final S states, and making modifications in the effective interaction Hamiltonian⁹ appropriate to the discussion of the cross section near threshold, one then obtains for $I(\theta, E_e')$

$$I(\theta, E_e') \rightarrow [(F_{1p} + F_{1n})^2 - 2(q/2m)^2(F_{1p} + F_{1n}) \times (\kappa_p F_{2p} + \kappa_n F_{2n}) + \frac{2}{3}(q/2m)^2[2 \tan^2(\frac{1}{2}\theta) + 1] \times (F_{1p} + F_{1n} + \kappa_p F_{2p} + \kappa_n F_{2n})^2] K_T^2 + \frac{1}{3}(q/2m)^2[2 \tan^2(\frac{1}{2}\theta) + 1] \times (F_{1p} - F_{1n} + \kappa_p F_{2p} - \kappa_n F_{2n})^2 K_S^2. \quad (33)$$

This expression may be further simplified if one uses the relations $F_{1p} \approx F_{2p} \approx F_{1n}$ and $F_{1n} \approx 0$ which are found experimentally to be valid over the range of q of present interest.⁴ The 3S_1 and 1S_0 matrix elements K_{101} and K_{000} will henceforth be denoted by K_T and K_S as above.

The matrix elements K_T and K_S have been calculated for the following two models of the deuteron and final S -state wave functions in addition to the Bargmann model:

$$\text{Hulthén: } u(r) = Ne^{-\alpha r}(1 - e^{-\gamma r}), \quad (34.1)$$

$$F_{S,T}(pr) = (1 - e^{-\lambda_S, Tr}) \sin(pr + \delta_{S,T}). \quad (34.2)$$

$$\text{Repulsive core: } u(r) = Ne^{-\alpha r}(1 - e^{-\gamma r}) \times (1 - e^{-\mu r})^2, \quad (35.1)$$

$$F_{S,T}(pr) = (1 - e^{-\lambda_S, Tr})(1 - e^{-\mu r})^2 \times \sin(pr + \delta_{S,T}). \quad (35.2)$$

The Hulthén model corresponds to a potential which is attractive and singular at the origin; the wave functions $u(r)$ and $F_{S,T}(pr)$ satisfy the usual boundary conditions at infinity, $u(r) \rightarrow Ne^{-\alpha r}$, $F_{S,T}(pr) \rightarrow \sin(pr + \delta_{S,T})$, and vanish linearly for $r \rightarrow 0$. The wave functions for the repulsive core model, on the other hand, vanish as r^3 for $r \rightarrow 0$, simulating thereby the effects of a strong repulsion between the nucleons with a range given roughly by $(2\mu)^{-1}$. When the re-

¹⁹ V. Bargmann, *Revs. Modern Phys.* **21**, 488 (1949).

maining parameters are properly chosen, the wave functions also satisfy the conditions imposed by the low-energy neutron-proton scattering data. Thus, each of the wave functions should reproduce the appropriate effective range. In addition, the functions $u(r)$ and $\cot\delta_T F_T(p\mathbf{r})$ are expected to have essentially the same shape inside the range of the neutron-proton forces. Within this range, the small positive or negative energies represented by p and α may be neglected relative to the potential energy, and the shape of the wave functions for small r is determined predominantly by the latter. The foregoing model wave functions have this property. For example, using the effective-range expansion for the cotangent of the phase shift,

$$\cot\delta_{S,T} = -(pa_{S,T})^{-1} + \frac{1}{2}pr_{0,S,T} + \cdots, \quad p \rightarrow 0, \quad (36)$$

one obtains for the Hulthén wave functions for small r

$$u(r) \rightarrow [1 - \alpha r + \cdots](1 - e^{-\gamma r}) \quad (37.1)$$

and

$$\cot\delta_T F_T(p\mathbf{r}) \rightarrow [1 - (r/a_T)](1 - e^{-\lambda_T r}), \quad r, p \rightarrow 0. \quad (37.2)$$

Since the triplet scattering length a_T is given approximately by $a_T^{-1} \approx \alpha$, it is evident that the adjustment of γ and λ_T to reproduce the triplet effective range $r_{0,T}$ will require $\gamma \approx \lambda_T$, and the bound and free wave functions will indeed be similar in shape for r small. The same form has been used for the singlet and triplet free state wave functions, since the corresponding potentials are thought to be rather similar in character.^{12,13} We have in particular used the same repulsive core parameter μ in each.

In the calculations which have been performed using the model wave functions, the parameter γ was determined by matching the deuteron wave function $u(r)$ to the triplet effective range. The extra parameter μ in the repulsive core wave functions was evaluated simultaneously by requiring that the calculated deuteron form factor $F_d(q^2)$,

$$F_d(q^2) = \int_0^\infty j_0(\frac{1}{2}qr) u^2(r) dr, \quad (38)$$

give a reasonable fit to the recent data of Friedman *et al.*⁷ on elastic electron-deuteron scattering. The value of μ so obtained was used in the free state wave functions $F_{S,T}(p\mathbf{r})$, and the remaining parameters $\lambda_{S,T}$ were matched to the appropriate effective ranges. In practice, it was found that a reasonable fit to F_d could be obtained with the repulsive core wave functions, but the precise value of μ depended rather sensitively on the experimental value taken for F_d and on the value of q at which the form factors were matched.²⁰ However, satisfactory

²⁰ In the course of the calculations, we attempted to fit the deuteron form factor F_d using for the deuteron wave function $u(r) = N e^{-\alpha r} (1 - e^{-\gamma r}) (1 - e^{-\mu r})$. The fit obtained with this wave function was not satisfactory, and it was necessary to add the extra factor of $(1 - e^{-\mu r})$ which appears in the wave function given in Eq. (35.1).

solutions of the combined matching problem (form factor and effective range) were found in the region $\gamma \approx \mu$. It was consequently assumed in the final calculations with the repulsive core wave functions that $\gamma = \mu$, and the single remaining parameter μ was determined from the triplet effective range. The resulting parameters in the two cases were as follows; Hulthén: $\gamma = 1.202 \text{ f}^{-1}$, $\lambda_S = 1.215 \text{ f}^{-1}$, $\lambda_T = 1.246 \text{ f}^{-1}$; repulsive core: $\gamma = \mu = 2.13 \text{ f}^{-1}$, $\lambda_S = 1.72 \text{ f}^{-1}$, $\lambda_T = 2.62 \text{ f}^{-1}$; $\alpha = 0.232 \text{ f}^{-1}$, $N^2 = 0.766 \text{ f}^{-1}$. The Hulthén and hard-core deuteron wave functions are shown in Fig. 5, while the deuteron form factors F_d^2 calculated for the two models are shown in Fig. 6 along with the data of Friedman *et al.*⁷ The theoretical form factor corresponding to the Hulthén wave function fails completely to fit the data, while that corresponding to the repulsive core wave function provides a reasonable fit. That the agreement of the theoretical and experimental results is not precise is to be expected, considering the crudity of the one parameter model for $u(r)$. The fit could undoubtedly be improved by going to a larger radius for the repulsive core. As may be seen from Fig. 5, the radius of an equivalent hard [infinitely repulsive] core is about 0.2 f in the present model. This is somewhat smaller than the radius 0.26–0.30 f indicated by the Gartenhaus wave function²¹ which was found by McIntyre *et al.*⁶ to give a good fit to F_d^2 . The curvature of F_d^2 could probably be corrected as well if the contributions of the deuteron D state were included, since these tend to increase F_d^2 .

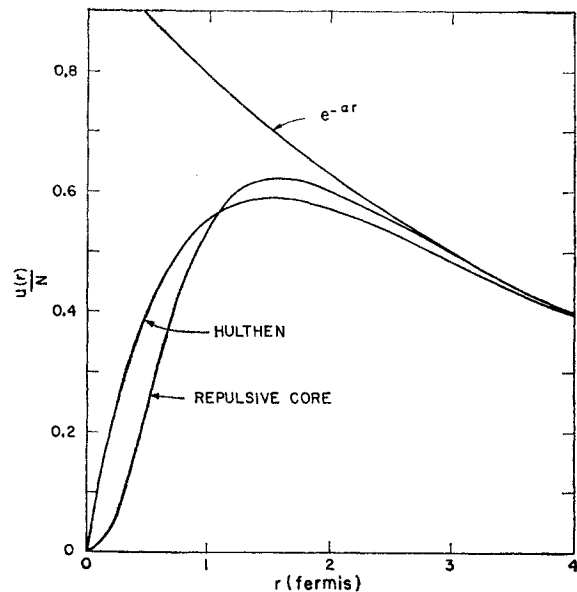


Fig. 5. Model wave functions for the deuteron. It is apparent that the repulsive-core and Hulthén wave functions differ insignificantly from the asymptotic wave function $e^{-\alpha r}$ for $r \gtrsim 4 \text{ f}$.

²¹ S. Gartenhaus, Phys. Rev. **100**, 900 (1955). The Signell-Marshak analysis of the nucleon-nucleon scattering data below 150 Mev¹³ is based on the Gartenhaus potential, with additional phenomenological spin-orbit potentials.

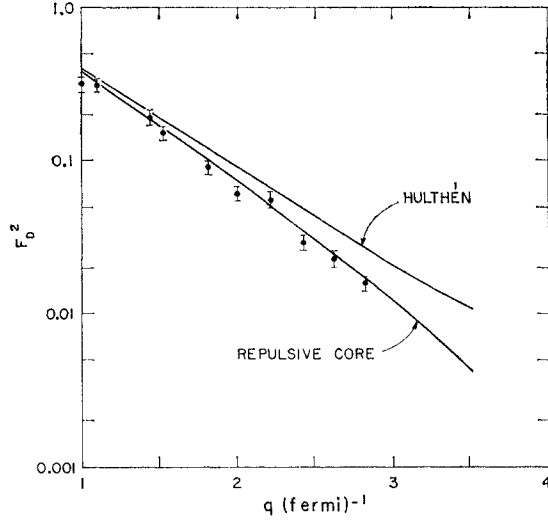


FIG. 6. Theoretical values of the square of the deuteron form factor F_d^2 calculated from the Hulthén and repulsive-core wave functions for the deuteron given in Eqs. (34) and (35). The experimental data are those of Friedman *et al.*⁷

for large values of q .⁶ It is in any case evident that the effects of the repulsive core cannot be neglected, and convenient to investigate these effects initially using relatively simple wave functions.

Calculation of the matrix elements K_S and K_T is straightforward and can be performed analytically using the simple wave functions discussed above. Some simplifications are nevertheless possible for the small values of p with which we are concerned. The typical integrals which enter $K_{S,T}$ for the model wave functions are of the form

$$\int_0^\infty j_0(\frac{1}{2}qr) \sin pr e^{-\nu r} dr = (2q)^{-1} \times \{ \ln[(\frac{1}{2}q+p)^2 + \nu^2] - \ln[(\frac{1}{2}q-p)^2 + \nu^2] \} \rightarrow p[\frac{1}{4}q^2 + \nu^2]^{-1}, \quad p \rightarrow 0, \quad (39)$$

and

$$\int_0^\infty j_0(\frac{1}{2}qr) \cos pr e^{-\nu r} dr = q^{-1} \times \{ \tan^{-1}[(\frac{1}{2}q+p)/\nu] + \tan^{-1}[(\frac{1}{2}q-p)/\nu] \} \rightarrow (2/q) \tan^{-1}(q/2\nu), \quad p \rightarrow 0. \quad (40)$$

In the present calculations, we have used the indicated limiting forms of the integrals for $p \rightarrow 0$; these are sufficiently accurate for the range of p which has been considered, $0 \leq p \leq 0.19$, f^{-1} the errors in each case being of relative order p^2 .²² It is convenient to introduce

²² For $p=0.10$ f^{-1} , $q=2.50$ f^{-1} , and the Hulthén-type wave functions of Eqs. (34), the approximate values of k_1 and k_2 were found to be respectively 0.9% and 0.3% smaller than the exact values for both the singlet and the triplet parameters. For the hard core wave functions, the approximate values were 1.6% and 0.3% small. The corresponding errors in $d^2\sigma/(d\Omega_e dE_s)$ were -0.6% for both the Hulthén and hard-core wave functions. The

functions $g_{1,i}(r)$ and $g_{2,i}(r)$ which approach unity for $r \rightarrow \infty$, and write $F_{S,T}(pr)$ in the form

$$F_i(pr) = \cos \delta_i g_{1,i}(r) \sin pr + \sin \delta_i g_{2,i}(r) \cos pr, \quad i=S,T. \quad (41)$$

The matrix elements $K_{S,T}$ are then given for small p by

$$K_i(p,q) \rightarrow 2N(pq)^{-1} \{ 2(p/q) \cos \delta_i(p) k_{1,i}(q) + \sin \delta_i(p) k_{2,i}(q) \}, \quad (42)$$

where

$$k_{1,i} = N^{-1} \int_0^\infty j_0(x) u(x) g_{1,i}(x) x dx \quad (43)$$

and

$$k_{2,i} = N^{-1} \int_0^\infty j_0(x) u(x) g_{2,i}(x) dx. \quad (44)$$

We have expressed the integrals in terms of the dimensionless quantity $x = \frac{1}{2}qr$ and have removed also the deuteron normalization factor $N = [2\alpha/(1 - \alpha r_{0,T})]^{1/2}$ to make $k_{1,i}$ and $k_{2,i}$ dimensionless. These functions depend on q alone; the entire dependence of the matrix elements on p is contained in the phase shifts and the factors of p which appear explicitly. The functions $k_{1,i}$ and $k_{2,i}$ were calculated for q in the range $1.5 \text{ f}^{-1} \leq q \leq 5.0 \text{ f}^{-1}$ for both the Hulthén and the repulsive core wave functions. The results are shown in Figs. 7 and 8 for the singlet

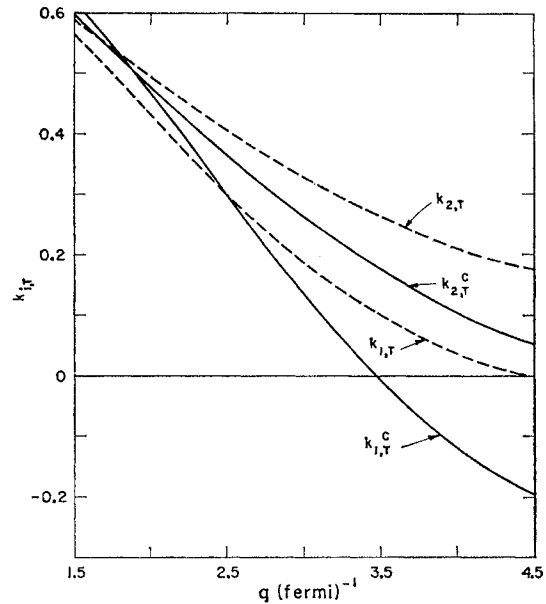


FIG. 7. Values of the dimensionless parameters $k_{1,S}(q)$ and $k_{2,S}(q)$ entering the definition of the singlet matrix element K_S , Eq. (42). The curves labeled by $k_{1,S}$ correspond to the Hulthén-type wave functions of Eqs. (34), those labeled by $k_{i,S}$ to the repulsive-core wave functions of Eqs. (35).

errors increase quadratically with p , reaching 2.5% for $p=0.20$ f^{-1} . However, the approximate cross sections integrated over the interval $0 \leq p \leq 0.20$ f^{-2} are only 0.8% too small, and the errors cancel out essentially completely in the ratio of the hard core to the Hulthén results. The errors increase slightly with increasing q , but remain small in the cross section and negligible in the ratio.

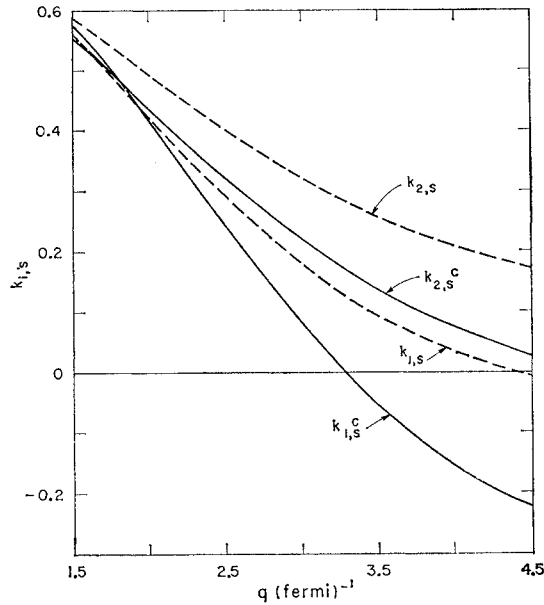


FIG. 8. Values of the dimensionless parameters $k_{1,T}(q)$ and $k_{2,T}(q)$ entering the definition of the triplet matrix element K_T , Eq. (42). The curves labeled by $k_{i,T}$ correspond to the Hulthén-type wave functions of Eqs. (34), those labeled by $k_{i,T}^c$, to the repulsive-core wave functions of Eqs. (35).

and triplet final states of the neutron-proton system. The K 's are considerably different for the two models, and it is apparent that the theoretical values of the cross section will also differ significantly, especially for large values of q . The complete integrand for K_S in the two models is shown in Fig. 9 for $p=0.10$ f $^{-1}$ and $q=2.50$ f $^{-1}$. The effects of the suppression of the repulsive core wave function for small values of r are clearly seen.

Similar calculations were carried out using the Bargmann wave functions¹⁹ in order that a comparison with the work of Jankus could be made. In this model, the deuteron wave function is given by

$$u(r) = N e^{-\alpha r} (1 - e^{-\lambda_T r}) (1 + \beta_T e^{-\lambda_T r})^{-1}, \quad (45)$$

while the free S -state wave functions are given by

$$F_i(pr) = \cos \delta_i (1 - \beta_i e^{-\lambda_i r}) (1 + \beta_i e^{-\lambda_i r})^{-1} \sin pr \\ + \sin \delta_i (1 - e^{-\lambda_i r}) (1 + \beta_i e^{-\lambda_i r})^{-1} \cos pr \\ + 8\beta_i p^2 [(4p^2 + \nu_i^2)(4p^2 + \lambda_i^2)]^{-1/2} e^{-\lambda_i r} \\ \times (1 + \beta_i e^{-\lambda_i r})^{-1} \sin pr, \quad (46)$$

where $i=S, T$, and $\lambda_S=1.57$ f $^{-1}$, $\lambda_T=1.96$ f $^{-1}$, $\beta_S=0.90$, $\beta_T=1.62$, and $\nu_i=\lambda_i(\beta_i-1)(\beta_i+1)^{-1}$. The Bargmann wave functions are reduced in magnitude for small r relative to the Hulthén-type wave functions of Eqs. (34), but not as much as the repulsive core wave functions of Eqs. (35). They therefore represent an intermediate case in the study of core effects. The last term in the expression for $F_i(pr)$ is very small for the range of p of present interest, and was neglected. The functions $k_{1,i}$ and $k_{2,i}$ were calculated by subtracting from the integrands their asymptotic forms for large r .

These terms could be integrated analytically, while the remainders, which vanished rapidly with increasing r , were integrated numerically. The resulting values of $k_{1,i}$ and $k_{2,i}$ were found to lie as expected between the values obtained for the other models.

Calculation of the angular distribution function $I(\theta, E_e')$, Eq. (33), in terms of the singlet and triplet phase shifts and the functions $k_{1,i}$ and $k_{2,i}$ is straightforward. We have assumed that $F_{1p}=F_{2p}=F_{2n}$, and that $F_{1n}=0$,⁴ the nucleon structure then affecting the results only through an over-all factor $(F_p)^2$. The quantity $pI(\theta, E_e')/(F_p)^2$ is shown in Fig. 10 for the following parameters: $E_e=500$ Mev, $E_0=393$ Mev, $\theta=90^\circ$, and $E_0-E_e' \leq 1.2$ Mev. The variation in q over this small range in E_e' is negligible, and q has therefore been given its value for $E_e'=E_0$, $q=3.20$ f $^{-1}$. The contribution of the 1S_0 final state for the nucleons is seen to be much larger than that of the 3S_1 final state for values of E_e' very close to E_0 . The sharp peak in the singlet contributions is easily understood. For p sufficiently small, $\cot \delta_S$ may be represented by the first term in the effective range expansion, Eq. (36), $\cot \delta_S \rightarrow -(pa_S)^{-1}$, and K_S is given approximately by

$$K_S \rightarrow 2N(pq)^{-1}(1+p^2a_S^2)^{-1/2} \\ \times \{2(p/q)k_{1,S} + [pa_S]k_{2,S}\}, \\ \frac{1}{2}(pr_{0,S})(pa_S) \ll 1. \quad (47)$$

As a consequence of the large magnitude of the singlet scattering length, $a_S=-23.8$ f,¹⁸ the quantity $2(p/q)k_{1,S}$

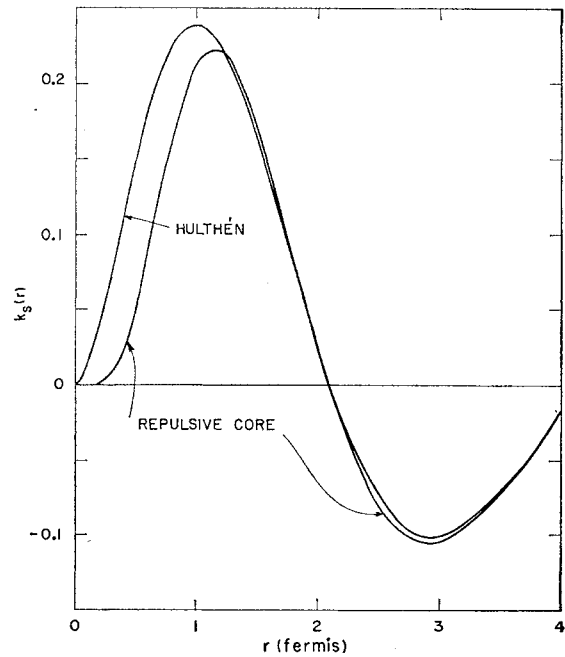


FIG. 9. Integrand for the singlet matrix element K_S calculated for the Hulthén-type and the repulsive-core wave functions of Eqs. (34) and (35) for $q=3.0$ f $^{-1}$ and $p=0.1$ f $^{-1}$. The singlet scattering phase shift for this value of p is 58° . The marked difference between the two wave functions for small r is clearly seen.

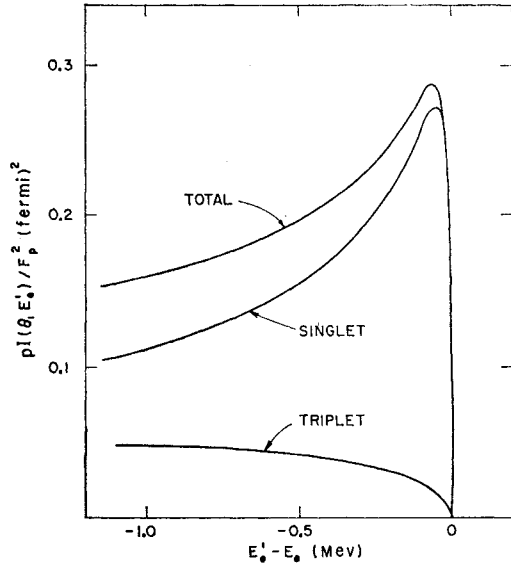


FIG. 10. The variation with E_e' of the function $pI(\theta, E_e')/F_p^2$ which determines the effects of the structure of the deuteron and final-state wave functions on $d^2\sigma/(d\Omega_e dE_e')$. The parameters are $E_e = 500$ Mev, $\theta = 90^\circ$, $E_0 = 393$ Mev, and the nominal value of q over this energy range is $q \approx 3.20$ f $^{-1}$. The sharp peaking in the contribution of the final 1S_0 state of the neutron-proton system is clearly seen. The repulsive-core wave functions of Eq. (35) were used in the calculation.

is always much smaller than $|pa_s|k_{2,s}$ for q in the range considered, $1.5 \text{ f}^{-1} \leq q \leq 4.5 \text{ f}^{-1}$ [see Fig. 7], and one obtains as a rough but useful approximation

$$K_S \approx 2N |a_s| q^{-1} (1 + p^2 a_s^2)^{-\frac{1}{2}} k_{2,s}. \quad (48)$$

The square of this matrix element appears in the function $pI(\theta, E_e')$ and in the cross-section $d^2\sigma/(d\Omega_e dE_e')$ multiplied by an extra factor of p . The resulting function $p|a_s|(1 + p^2 a_s^2)^{-1}$ vanishes for $p=0$, attains its maximum value for $p = |a_s|^{-1} = 0.042 \text{ f}^{-1}$, and drops again to one half of its maximum value for $p = 0.16 \text{ f}^{-1}$. Since $E_0 - E_e'$ is proportional to p^2 , the region of rapid variation of the singlet contributions to $pI(\theta, E_e')$ is compressed in the energy variable into a small range of final energies near E_0 , and the function $pI(\theta, E_e')$ appears sharply peaked in this energy range in Fig. 10. Similar considerations apply to the triplet contributions to $pI(\theta, E_e')$, but since the triplet scattering length is relatively small, $a_T = 5.38 \text{ f}$,¹⁸ the peaking is less prominent, and is not apparent for the limited range of energies shown in Fig. 10. From the considerations which lead to the approximation of Eq. (42) for the matrix elements $K_{S,T}$, it is evident both that the appearance of a peak in the cross section for $E_e' \approx E_0$ is essentially independent of the model used for the deuteron and free state wave functions, and that its shape is determined mainly by the known neutron-proton S -wave scattering phase shifts. Considerable information about the details of the wave functions is

nevertheless reflected in the magnitude and the finer details of the shape of the cross section.

The predicted peak in the cross-section $d^2\sigma/(d\Omega_e dE_e')$ was clearly observed in the experiments of Kendall *et al.*¹⁰ However, the measured values of $d^2\sigma/(d\Omega_e dE_e')$ were found to be smaller for large q than was expected on the basis of the Jankus theory.⁸ The ratio of the measured to the predicted cross section, each integrated over the interval $E_0 - E_e' \lesssim 1$ Mev, is shown in Fig. 4. The extent to which the neglect in the Jankus calculations of the effects of the repulsive core in the neutron-proton interaction accounts for the discrepancy may be determined by calculating the ratio of the integrated cross sections for the repulsive core to the Bargmann (Jankus) model. The integrated cross section is given by

$$\int_{E_0 - \Delta E}^{E_0} d^2\sigma/(d\Omega_e dE_e') = \sigma_{\text{Mott}}(2/\pi) \bar{I}(\theta, E_e, \Delta E) \times [1 + (E_e/m) \sin^2(\frac{1}{2}\theta)]^{-1}, \quad (49)$$

where

$$\bar{I}(\theta, E_e, \Delta E) = \int_0^{p_m} I(\theta, E_e') p^2 dp, \quad (50)$$

and p_m is the maximum included value of the momentum p , corresponding to the minimum value of E_e' , $E_e' = E_0 - \Delta E$.²³ The desired ratio of the cross sections is given by the ratio of the functions \bar{I} for the two models. Since q does not vary significantly for $\Delta E \lesssim 1$ Mev, the functions $k_{1,i}$ and $k_{2,i}$ as well as the factors of q which appear in Eq. (33) may be regarded as constants as far as the above integration is concerned. The entire dependence of $I(\theta, E_e')$ on p then arises from the phase shifts and kinematical factors which appear in the definition of the matrix elements $K_{S,T}$, Eq. (42). The required integrals are easily performed analytically using the effective range expansion given in Eq. (36) to determine the phase shifts.

The calculated values of the dimensionless quantity $\bar{I}(\theta, E_e, \Delta E) \cos^2(\frac{1}{2}\theta)/F_p^2$ are shown in Fig. 11 for $E_e = 500$ Mev and $\Delta E = 1$ Mev. The predictions of the three different models differ drastically for large values of θ [large values of q], the repulsive core wave functions leading as expected to the smallest results. The ratios of the repulsive core values of \bar{I} to the values for the Hulthén and Bargmann (Jankus) models are shown in Fig. 4 along with the experimental-to-Jankus ratios determined by Kendall *et al.*¹⁰ It is seen that the general trend of the experimental-to-Jankus ratio is reproduced by the repulsive core model, even though the wave functions are somewhat inaccurate as indicated by the lack of precision in the fit to F_d [see Fig. 6]. It in any case seems clear that the discrepancy with the Jankus theory found by Kendall *et al.*¹⁰ can be accounted for

²³ Note that for fixed values of E_e and θ , the quantities q , p , and E_e' are all determined if the value of any one is given. It is convenient for the present purposes to take the minimum value of E_e' , or ΔE , as the independent variable.

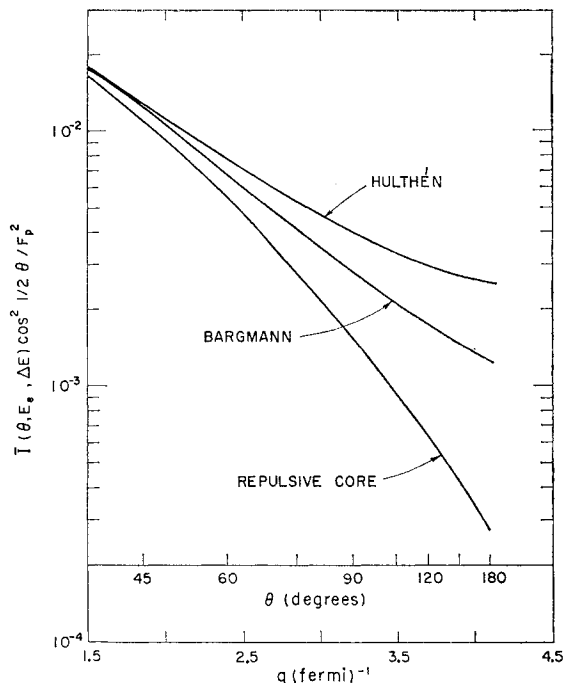


FIG. 11. Values of the function $[\bar{I}(\theta, E_e, \Delta E) \cos^2(\frac{1}{2}\theta)]/F_p^2$ defined in Eq. (50). This function contains the effects on the integrated cross section of the structure of the deuteron and final-state wave functions. The parameters used were $E_e = 500$ Mev and $\Delta E = 1$ Mev. The Bargmann wave functions were used in the calculations of Jankus.⁸ The Hulthén-type and repulsive-core wave functions of the present paper are defined in Eqs. (34) and (35).

by using in the calculation of the matrix elements $K_{S,T}$ wave functions which take adequate account of the repulsive core in the neutron-proton interaction.

From the foregoing results, it is evident that the study of the inelastic electron-deuteron scattering cross sections near the threshold can, in principle, provide important new information concerning the structure at small distances of the 3S_1 and 1S_0 free state wave functions of the neutron-proton system. Analogous information about the deuteron wave function has already been obtained from measurements of the elastic scattering cross sections.⁶ It should nevertheless be recognized that the semirelativistic theory is open to question in both cases for the large momentum transfers which are of interest. The important configurations for the scattering near threshold are those in which the nucleons are close together, and one may correspondingly expect the contributions of meson currents to the scattering to be important. The nucleons are furthermore considerably off the mass shell, with the consequence that the measured form factors could in any case differ significantly from the free nucleon form factors. These questions can probably be best examined using the methods of relativistic dispersion theory, as sketched in the next Section. It is perhaps a hopeful sign that, in the case of elastic scattering, the relevant dispersion re-

lation has an anomalous threshold, with a weight function in the anomalous region which is closely related to the nonrelativistic deuteron wave function.²⁴ Anomalous threshold are again present in the case of inelastic scattering, and it is likely that the Mandelstam spectral function in the anomalous region can again be related to the nonrelativistic wave functions; but this has not yet been verified. In the absence of a detailed relativistic calculation, including mesonic effects, it is not certain that the effects here attributed to a repulsive core in the two-nucleon interaction cannot be ascribed to other sources, but we shall retain this interpretation in the remainder of the discussion. The approximations which led to Eq. (42) for small values of p are expected to be valid for any reasonable wave functions, the detailed structure of which is implicit in the functions $k_{1,i}(q)$ and $k_{2,i}(q)$. Since q does not vary significantly over a small range of energies, the k 's may be considered as constants in any given experiment with fixed E_e and θ , and with $E_0 - E_e'$ small. While it is in principle possible to determine these constants by a detailed study of the shape of the cross section $d^2\sigma/(d\Omega_e dE_e')$ near threshold, the scattering phase shifts being known, such an analysis is complicated by the smearing out of the cross section associated with the finite energy resolutions encountered experimentally, and appears to be very difficult to carry out. We remark, however, that the cross section depends primarily on the functions $k_{2,i}$. It may therefore be possible to determine from the experiments of Kendall *et al.*¹⁰ the variation with q of these functions by assuming the less important functions $k_{1,i}$ to be known. Separate evaluation of $k_{2,S}$ and $k_{2,T}$ would provide directly information on the difference between the singlet and triplet wave functions, hence, between the corresponding potentials, for small internucleon separations. This information cannot at present be obtained with any certainty from other sources. Alternatively, the experiments of Kendall *et al.*¹⁰ can be used as a test of present ideas regarding the two-nucleon interaction.¹²⁻¹⁴ It would be desirable from this point of view to calculate the matrix elements $K_{S,T}$ using wave functions corresponding to the present semi-phenomenological potentials, preferably including the effects of the D -state components of the deuteron and the free ($^3S_1 + ^3D_1$) wave functions which have here been omitted. The work of McIntyre and Dhar⁶ on the deuteron form factor F_d indicates that these effects will be significant for large values of q . Finally, it is interesting to note that the inelastic electron-deuteron scattering process considered here represents an extension to virtual photon momenta of the photodisintegration of the deuteron. Detailed calculations of the latter process using wave functions from the semi-phenomenological potentials have been markedly successful for photon

²⁴ R. Blankenbecler and Y. Nambu, *Nuovo cimento* **18**, 595 (1960).

energies up to 150 Mev;²⁵ it will be interesting to see if the same agreement between theory and experiment can be obtained in the present case, where the important matrix elements are quite different.

IV. REMARKS ON THE RELATIVISTIC THEORY OF INELASTIC ELECTRON-DEUTERON SCATTERING

Relativistic corrections to the cross sections for inelastic electron-deuteron scattering were considered in Appendix I of (I).⁹ However, that treatment of relativistic effects was not completely satisfactory, since the description of the deuteron wave function used in (I) was inherently noncovariant. We wish in this section to examine more thoroughly the relativistic theory of inelastic electron-deuteron scattering using the techniques of dispersion relations. Since the two-nucleon system is assumed to interact only once with the electron, the basic problem is the calculation of the transition amplitude $(2\pi)^4 \delta^4(p+n-d-q) \langle np | j_\mu | d \rangle$, where j_μ is the electromagnetic current operator, q is the electron 4-momentum transfer $q=e-e'$, and the nucleon and deuteron 4-momenta are denoted by the particle labels. On the basis of the singularities found in perturbation theory,²⁶ this amplitude is expected to satisfy a Mandelstam representation with a normal threshold in the center-of-mass energy variable $s=-(d+q)^2=-(p+n)^2$, and with anomalous thresholds in both the momentum transfer variables $t=-(d-n)^2$ and $u=-(d-p)^2$. The representation consists of single dispersion integrals and pole terms in each of the variables s , t , and u separately, and double dispersion integrals in the three pairs of variables. The existence of such a representation provides in principle a powerful tool for the study of relativistic and mesonic corrections to the simple theory of inelastic electron-deuteron scattering considered in the preceding sections; but as a practical matter, it is the importance of the pole terms and the possibility of connecting the spectral functions in the anomalous regions with the nonrelativistic wave functions which make a detailed calculation relatively simple. We shall consequently devote most of the following discussion to these simple connections between the relativistic and nonrelativistic theories. A number of corrections to the latter will be estimated, and the general outline of a complete calculation of $\langle np | j_\mu | d \rangle$ will be sketched, but detailed calculations will be reserved for a later paper.

a. Pole Terms in the Single Dispersion Relations

For momenta corresponding to the quasi-elastic peak in the cross-section $d^2\sigma/(d\Omega dE_e')$, the dominant con-

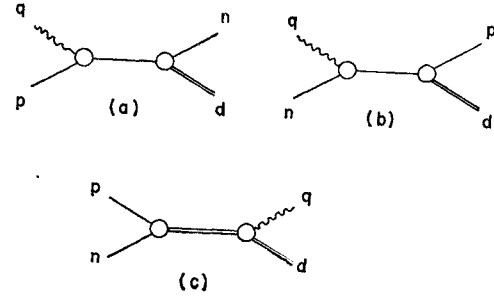


FIG. 12. Diagrams corresponding to the pole terms in the dispersion relations for the transition amplitude $\langle np | j_\mu | d \rangle$.

tributions to $\langle np | j_\mu | d \rangle$ are associated with the proton and neutron pole terms in the single dispersion relations in t and u , respectively. It is, therefore, of interest to study these terms in detail before considering more complicated contributions. The corresponding diagrams for the absorptive parts are shown in Figs. 12(a) and 12(b). The nucleon-photon vertex in Figs. 12(a) and 12(b) involves just the nucleon form factors for particles on the mass shell. For example, in Fig. 12(a), the proton vertex function is given by

$$\langle p | j_\mu(0) | p' \rangle = -ie(4p_0 p'_0)^{-\frac{1}{2}} \bar{u}(p) \times [\gamma_\mu F_1(q^2) + (\kappa_p/2m) \sigma_{\mu\nu} q_\nu F_2(q^2)] u(p'), \quad (51)$$

where $q=p'-p$, and the spinors are normalized as $\bar{u}(p)\gamma_\mu u(p)=2ip_\mu$. The neutron-proton-deuteron vertex has been studied by Blankenbecler *et al.*,²⁷ who show that for all particles on the mass shell, it has the form

$$\bar{u}(p) \langle n | f_p(0) | d \rangle = (8p_0 n_0 d_0)^{-\frac{1}{2}} \bar{u}(p) \times [F(m^2) i\gamma \cdot \xi + G(m^2) n \cdot \xi] u^c(n). \quad (52)$$

Here $f_p(0)$ is the proton current operator, ξ is a complex spacelike polarization vector describing the deuteron spin, $\xi \cdot d=0$, $u^c(n)=[\bar{u}(n)C]^T$, and C is the charge conjugation matrix. F and G are form factors for the deuteron vertex, and are functions of $t=-(d-n)^2$ for the proton off the mass shell. However, only the values of these functions for $t=m^2$ are involved in the contributions to the pole diagram of Fig. 12(a). The values of $F(m^2)$ and $G(m^2)$ were determined by Blankenbecler *et al.*²⁷ by considering the nonrelativistic limit of Eq. (52). For the standard normalization of the deuteron wave function,

$$\int_0^\infty [u^2(r) + w^2(r)] dr = 1, \quad (53)$$

$F(m^2)$ and $G(m^2)$ were found to be

$$F(m^2) = (8\pi/m)^{\frac{1}{2}} [1 + (1/\sqrt{2})\rho] N(1+\rho^2)^{-\frac{1}{2}}, \quad (54.1)$$

$$G(m^2) = (36\pi/m^2)^{\frac{1}{2}} \rho N(1+\rho^2)^{-\frac{1}{2}}, \quad (54.2)$$

²⁵ J. J. deSwart and R. E. Marshak, Phys. Rev. **111**, 272 (1958). W. Zernik, M. L. Rustgi, and G. Breit, *ibid.* **114**, 1358 (1959). M. L. Rustgi, W. Zernik, G. Breit, and D. J. Andrews, *ibid.* **120**, 1881 (1960).

²⁶ R. Karplus, C. M. Sommerfield, and E. M. Wichmann, Phys. Rev. **111**, 1187 (1958); **114**, 376 (1959). S. Mandelstam, *ibid.* **115**, 1741 (1959). J. Tarski, J. Math. Phys. **1**, 149 (1960).

²⁷ R. Blankenbecler, M. L. Goldberger, and F. R. Halpern, Nuclear Phys. **12**, 629 (1959). M. L. Goldberger, Y. Nambu, and R. Oehme, Ann. Phys. **2**, 226 (1957).

where

$$N = [2\alpha/(1-\alpha r_0)]^{\frac{1}{2}}, \quad (55)$$

and ρ is the ratio of the asymptotic D to S -state radial wave functions, $\rho \approx 0.03$.¹⁸ Combining the foregoing results, one obtains immediately for the contribution to the transition matrix element of the proton pole term

$$\langle n\mathbf{p} | j_\mu | d \rangle_{\text{proton pole}} = e(8p_0 n_0 d_0)^{-\frac{1}{2}} \times [(d-n)^2 + m^2]^{-1} J_\mu^p(p, n), \quad (56.1)$$

where

$$J_\mu^p(p, n) = \bar{u}(p) [\gamma_\mu F_1(q^2) + (\kappa_p/2m) \sigma_{\mu\nu} q_\nu F_2(q^2)] [-i\gamma \cdot (d-n) + m] \times [F(m^2) i\gamma \cdot \xi + G(m^2) n \cdot \xi] u^c(n). \quad (56.2)$$

A term of similar structure is obtained for the neutron pole diagram, Fig. 12(b), but the dispersion variable is now $u = -(d-p)^2$ rather than t .

The significance of the nucleon pole terms is easily seen. In the nonrelativistic theory of inelastic electron-deuteron scattering without final state interactions, the deuteron wave function enters that part of the transition matrix element corresponding to the interaction of the electron with the proton, through the Fourier-Bessel transform

$$F(\theta) = \int_0^\infty j_0(|\mathbf{n}|r) u(r) r dr, \quad (57)$$

where \mathbf{n} is the final laboratory momentum of the neutron [see Eqs. (15)]. If the deuteron wave function is replaced by its asymptotic form $N e^{-\alpha r}$, one obtains the approximate result

$$F(\theta) \approx N[\alpha^2 + \mathbf{n}^2]^{-1}. \quad (58)$$

This factor in the transition matrix element is reproduced, along with relativistic corrections, by the denominator in the proton pole term, Eq. (56.1). Extracting the corresponding normalization factors from $F(m^2)$, and evaluating the quantity $[(d-n)^2 + m^2]^{-1}$ in the deuteron rest frame, one obtains

$$2N[(d-n)^2 + m^2]^{-1} = N[Mn_0 - \frac{1}{2}M^2]^{-1} = N[\alpha^2 + \mathbf{n}^2(1 - \mathbf{n}^2/4m^2 + \dots)]^{-1}, \quad (59)$$

$$d = (0, M),$$

where we have used the relation $\alpha^2 = m\epsilon$, with ϵ the binding energy of the deuteron. It is interesting to note that the extra terms in the denominator in Eq. (59), representing relativistic corrections to the result of Eq. (58), can be obtained to the order shown by calculating the asymptotic deuteron wave function from a semi-relativistic equation of the Breit type.²⁸ In the

²⁸ G. Breit, Phys. Rev. **34**, 553 (1929). An approach to the relativistic theory of inelastic electron-deuteron scattering using Breit-type wave functions for the deuteron was discussed in Appendix I of reference 9. However, the extra terms $\mathbf{n}^2 \rightarrow \mathbf{n}^2 \times (1 - \mathbf{n}^2/4m^2 + \dots)$ noted in Eq. (57) were unfortunately omitted in the definition of the function $F_r(\theta)$.

calculation of the cross-section $d^2\sigma/(d\Omega dE_e')$, it is necessary to integrate over the angular distribution of the emerging nucleons. Re-expressing the quantity $2N[(d-n)^2 + m^2]^{-1}$ in the center-of-mass system of the outgoing nucleons, $\mathbf{p} + \mathbf{n} = \mathbf{d} + \mathbf{q} = 0$, we obtain

$$2N[(d-n)^2 + m^2]^{-1} = N[\alpha^2 + p^2 + \frac{1}{4}q^2 - \mathbf{p} \cdot \mathbf{q}]^{-1}, \quad (60.1)$$

where q^2 is the square of the electron 4-momentum transfer, $p = |\mathbf{p}|$ is the momentum of the proton in the center-of-mass system, and \mathbf{q} is the electron 3-momentum transfer in that system,

$$|\mathbf{q}|^2 = q^2 + [\frac{1}{4}q^2 - p^2 - \alpha^2]/(m^2 + p^2). \quad (60.2)$$

The expression of Eq. (60.1) enters the cross-section $d^2\sigma/(d\Omega dE_e')$ squared and integrated over the direction of \mathbf{p} . The resulting function evidently attains its maximum value, which corresponds to the quasi-elastic peak in the cross section, for $p^2 = \frac{1}{4}q^2$. It should be noted that the timelike component of q is then essentially zero in the center-of-mass system of the nucleons, $q \rightarrow (\mathbf{q}, 0)$, $\mathbf{q}^2 \rightarrow q^2$. The nonrelativistic analog of Eq. (60.1) is obtained by replacing the laboratory momentum of the neutron \mathbf{n} in Eq. (58) by the nonrelativistic expression $\mathbf{n} = \frac{1}{2}\mathbf{q}' - \mathbf{p}$, where \mathbf{q}' is the electron 3-momentum transfer in the laboratory system:

$$N[\alpha^2 + \mathbf{n}^2]^{-1} = N[\alpha^2 + p^2 + \frac{1}{4}q'^2 - \mathbf{p} \cdot \mathbf{q}']^{-1}. \quad (61)$$

While this result is similar in form to that given in Eq. (60.1), the predicted position of the quasi-elastic peak is determined by the condition $p^2 = \frac{1}{4}q'^2$ rather than $p^2 = \frac{1}{4}q^2$, the predicted peak energy being too low whether or not p is calculated relativistically. We may remark, however, that the *ad hoc* replacement of \mathbf{q}'^2 by q^2 used by Yearian and Hofstadter⁴ to bring the Jankus theory⁸ into better agreement with experiment leads according to Eqs. (60) to the correct result at the peak. However, the replacement is not valid for other values of E_e' .

The contribution to the cross-section $d^2\sigma/(d\Omega dE_e')$ of the pole terms could in principle be calculated in full detail (Bose²⁹ has in fact calculated the contribution of

²⁹ S. K. Bose, Nuovo cimento (to be published). Bose has proposed that the neutron magnetic form factor be determined by a Chew-Low type of extrapolation to the neutron pole. The pole terms in fact dominate the cross section $d^2\sigma/(d\Omega dE_e')$ at the quasi-elastic peak; the use of the complete deuteron wave function in the calculation of the function $M(p, q)$, Eqs. (29) and (31), leads to results about 16% smaller than would be obtained from the pole terms (asymptotic deuteron wave function) alone. On the other hand, the advantage of the small extrapolation distance is off set by the necessity of detecting one of the emerging nucleons in coincidence with the scattered electron. The subsequent possibilities are as follows: (1) measurement of the neutron angular distribution and extrapolation in the angle relating its direction in the center-of-mass system to the direction \hat{q} ; (2) measurement of the energy of the emerging (low energy) proton and extrapolation in p^2 to the pole at $p^2 = -\alpha^2$; (3) measurement of the neutron energy with sufficient accuracy that $|\mathbf{p}|$ can be calculated. Possibilities (2) and (3) are remote, but (1) may be feasible. It may be worth remarking that the extrapolation can be considerably simplified if the influence of the nearby anomalous branch cuts are taken partially into account. This may be done fairly effectively by re-

the neutron magnetic moment scattering), but the calculations are lengthy, and the significance of various terms in the results is not especially clear. It is instead convenient to make a simplifying approximation before proceeding further. We note that at the quasi-elastic peak in the cross section, essentially the entire electron momentum transfer is absorbed by a single nucleon, the second nucleon emerging with a very small momentum in the laboratory system [deuteron rest system]. In fact, on the basis of the nonrelativistic theory with a Hulthén wave function for the deuteron, the average kinetic energy of the spectator nucleon is on the order of 5 Mev for the momentum transfers of present interest. It is therefore reasonable as a first approximation to evaluate the spin-dependent factors J_μ in the numerators of the pole terms on the assumption that the spectator nucleon is rigorously at rest in the laboratory system. Since the "scattered" nucleon is then initially at rest also, it is evident that the kinematical factors in the cross section which arise from these factors should be identical with those which occur in the cross sections for elastic electron-nucleon scattering. That this is true is easily verified.

The spin-dependent factor $J_\mu^p(p, n)$ in Eq. (56) simplifies considerably when one uses the relations

$$(-i\gamma \cdot n + m)u^c(n) = 0$$

and $\xi \cdot d = 0$, and specializes to the case $n = (0, m)$, $p = (\mathbf{q}, p_0)$, $d = (0, M) \simeq (0, 2m)$; then

$$J_\mu^p(p, n) \rightarrow 2imF(m^2)\bar{u}(\mathbf{q}, p_0)[\gamma_\mu F_1(q^2) + (\kappa_p/2m)\sigma_{\mu\nu}q_\nu F_2(q^2)]\gamma \cdot \xi u^c(0, m). \quad (62)$$

The contribution of the proton pole term to the cross-section $d^2\sigma/(d\Omega_e dE_e')$ involves the absolute square of J_μ^p , summed and averaged over the final and initial spins. However, when the average over the deuteron spin ξ is performed, the quantity which remains is identical aside from an overall factor to that encountered in the calculation of the scattering of electrons from protons initially at rest, the dependence of the transition matrix element on the proton spin being given in that case by a factor

$$\bar{u}(\mathbf{q}, p_0)[\gamma_\mu F_1(q^2) + (\kappa_p/2m)\sigma_{\mu\nu}q_\nu F_2(q^2)]u(0, m).$$

The expression for J_μ^p in Eq. (62) may be further simplified, and the connection of the relativistic with the nonrelativistic theory examined, by introducing two-component spinors for the nucleons through the

placing the single denominator $[(d-n)^2 + m^2]^{-1}$ in Eq. (56) by the combination $(\nu^2 - m^2)[(d-n)^2 + m^2]^{-1}[(d-n)^2 + \nu^2]^{-1}$, where $\nu^2 - m^2 = 2(\beta^2 - \alpha^2)$, and α, β are the parameters of a Hulthén model for the deuteron wave function. The extrapolation using this modified function should be linear for all practical purposes (see Sec. IVb). The approach of the present paper is to exploit the dominance of the pole terms to obtain a reliable theoretical calculation of the cross section in order that information on the neutron form factors may be extracted from the much less difficult measurements of $d^2\sigma/(d\Omega_e dE_e')$.

relations

$$u(\mathbf{q}, p_0) = (p_0 + m)^{\frac{1}{2}} \begin{pmatrix} 1 \\ \boldsymbol{\sigma} \cdot \mathbf{q} / (p_0 + m) \end{pmatrix} \chi_p, \quad (63.1)$$

$$u^c(0, m) = (2m)^{\frac{1}{2}} \begin{pmatrix} 0 \\ -i\sigma_2 \end{pmatrix} \chi_n, \quad (63.2)$$

where the γ matrices are used in the Dirac representation with $C = \gamma_2 \gamma_4 = i\alpha_2$. Omitting in the results terms involving powers of m^{-1} higher than the second, one then obtains

$$J_4^p \approx -4m^2 i F(m^2) [F_{1p} - (q^2/8m^2) \times (2\kappa_p F_{2p} - F_{1p})] \chi_p^* \boldsymbol{\sigma} \cdot \xi \sigma_2 \chi_n^{*T}, \quad (64.1)$$

and

$$\mathbf{J}^p \approx -2mi F(m^2) \chi_p^* [(F_{1p} + \kappa_p F_{2p}) \boldsymbol{\sigma} \times \mathbf{q} - i\mathbf{q} F_{1p}] \boldsymbol{\sigma} \cdot \xi \times \sigma_2 \chi_n^{*T}. \quad (64.2)$$

The results assume a more familiar form when the deuteron and the final spin states are represented by two-particle spin functions $\chi_{s^m}(s_p, s_n)$,

$$J_4^P \approx -4m^2 \sqrt{2} F(m^2) \chi_{s^m}' \times [F_{1p} - (q^2/8m^2)(2\kappa_p F_{2p} - F_{1p})] \chi_{1^m} \quad (65.1)$$

and

$$\mathbf{J}^p \approx -2m \sqrt{2} F(m^2) \chi_{s^m}' \times [(F_{1p} + \kappa_p F_{2p}) \boldsymbol{\sigma}_p \times \mathbf{q} - i\mathbf{q} F_{1p}] \chi_{1^m}. \quad (65.2)$$

The two terms in \mathbf{J}^p correspond to the interaction of the proton total magnetic moment and convection current with the field of the scattered electron, and appear in the present form in the non-relativistic Hamiltonian used by Jankus.⁸ On the other hand, the extra term $-(q^2/8m^2)(2\kappa_p F_{2p} - F_{1p})$ in J_4^p represents a relativistic correction to the effective charge, as was noted in (I).³⁰ The foregoing effective current, generalized to include the neutron contributions, was used in the calculations discussed in Secs. I and II. On the other hand, such a reduction is not necessary when the effects of final state interactions between the nucleons are neglected. The kinematical factors which appear in Eq. (15.1) multiplying the functions $M(p, q)$ and $N(p, q)$ were obtained using J_μ^p as given in Eq. (62). The error incurred at the quasi-elastic peak by neglecting in J_μ the momentum and kinetic energy of the spectator nucleon has been investigated, and was found to be entirely negligible.

We have so far neglected the deuteron pole term, Fig. 12(c) which appears in the single dispersion relation in the variable $s = -(d+q)^2 = -(p+n)^2$. The absorptive part for this term involves, in addition to the proton-

³⁰ The effective interaction Hamiltonian given in (I), Eqs. (2) and (6), involves the combination $(q^2/8m^2)(2\kappa_p F_{2p} + F_{1p})$ in the effective charge rather than the combination given above where F_{1p} appears with the opposite sign. However, as noted in (I), the convection current term which appears in Eq. (65.2) was also omitted; the results obtained from the two, seemingly inequivalent, currents are in fact identical to order m^{-2} . The form given in Eq. (65.2) is correct; that used in (I) is a convenient approximation.

neutron-deuteron vertex factor of Eq. (52), the deuteron electromagnetic vertex function

$$\begin{aligned} \langle d' | j_\mu | d \rangle = & e(4d_0 d_0')^{-\frac{1}{2}} [F_{1d}(q^2) \xi'^* \cdot \xi (d+d')_\mu \\ & + F_{2d}(q^2) (\xi_\mu \xi'^* \cdot q - \xi'^*{}_\mu \xi \cdot q) \\ & + F_{3d}(\xi'^* \cdot q \xi \cdot q / m^2) (d+d')_\mu]. \quad (66) \end{aligned}$$

The form factors F_{1d} are normalized for $q^2 \rightarrow 0$ according to the relations $F_{1d} \rightarrow 1$, $F_{2d} \rightarrow \mu_d$, and $F_{3d} \rightarrow Q + \frac{1}{2}(\mu_d - 1)$, where μ_d is the deuteron magnetic moment in units of the nuclear magneton, and Q is the quadrupole moment in units of m^{-2} . We will consider only the deuteron charge scattering, since this illustrates adequately the significance of the deuteron pole term. The corresponding contribution to the transition matrix element is then

$$\begin{aligned} \langle np | j_\mu | d \rangle_{\text{deuteron pole}} = & e(8p_0 n_0 d_0)^{-\frac{1}{2}} \\ & \times [(d+q)^2 + M^2]^{-1} (2d+q)_\mu F_{1d}(q^2) \bar{u}(p) \\ & \times [F(m^2) \gamma \cdot \xi - \frac{1}{2} G(m^2) (n-p) \cdot \xi] u^c(n). \quad (67) \end{aligned}$$

It is evident from the observation that the deuteron in the intermediate state in Fig. 12(c) is at rest in the center-of-mass system $\mathbf{p} + \mathbf{n} = 0$, that the transition matrix element of Eq. (67) leads only to final states of the two nucleon system with $J=1$ and even parity, that is, to final 3S_1 and 3D_1 configurations. Comparison of Eqs. (15b) and (67) shows the contribution of the deuteron pole term to the total transition matrix element $\langle np | j_\mu | d \rangle$ to be relatively unimportant at the quasi-elastic peak. It nevertheless represents a significant addition to the partial wave transition matrix elements leading to the 3S_1 and 3D_1 states, and is in fact associated in part with the correction to those matrix elements for the effect of interactions between the outgoing nucleons. [Additional corrections arise from the double dispersion relation in the Mandelstam representation for $\langle np | j_\mu | d \rangle$.] On the other hand, the deuteron pole term gives the dominant contribution to the matrix element near the threshold for deuteron breakup. The appearance in the numerator in Eq. (67) of the deuteron form factor F_{1d} is not unexpected in this region on the basis of the remarks which follow Eqs. (35) concerning the shapes of the deuteron and free 3S_1 wave functions for $p \rightarrow 0$. However, we will not at this time undertake a detailed calculation within the context of dispersion theory of the effects of final-state interactions in the scattering, but will instead rely on the wave function calculations discussed in Secs. I-III. The deuteron pole term will therefore be neglected in the ensuing discussion.

b. Single Dispersion Relations

The one-particle singularities of the transition amplitude $\langle np | j_\mu | d \rangle$ other than the simple pole terms lead to the appearance of single dispersion integrals in the variables s , t , and u . We will consider in detail only the t channel; essentially the same analysis holds for the u

channel, while the extra contributions in the s channel are of interest only for those transitions which lead to final 3S_1 or 3D_1 configurations for the nucleons. The one-particle singularities of $\langle np | j_\mu | d \rangle$ in the t channel arise in perturbation theory [treating the deuteron as an elementary vector particle] from those Feynman graphs which may be separated into two parts by cutting a single proton line. The total contribution to $\langle np | j_\mu | d \rangle$ of all such graphs may be expressed in terms of the complete proton propagator S_F' , and truncated vertex functions $\Gamma_\mu^{(p)}$ and Γ_d describing the proton electromagnetic vertex and the neutron-proton-deuteron vertex for the proton off the mass shell,

$$\begin{aligned} \langle np | j_\mu | d \rangle_{\text{single proton}} = & (8p_0 n_0 d_0)^{-\frac{1}{2}} \bar{u}(p) \Gamma_\mu^{(p)}(q, d-n) \\ & \times S_F'(d-n) \Gamma_d(d-n) u^c(n). \quad (68) \end{aligned}$$

The truncated vertex functions, which are equivalent to the vertex functions of Lehmann *et al.*³¹ when the latter are evaluated with two particles on the mass shell, may be obtained from the functions $\langle p | j_\mu | d-n \rangle$ and $\langle n | f_p | d \rangle$ by removing all components which are single-particle reducible with respect to the off-shell proton,

$$\begin{aligned} \langle p | j_\mu | d-n \rangle = & (2p_0)^{-\frac{1}{2}} \bar{u}(p) \Gamma_\mu^{(p)}(q, d-n) \\ & \times S_F'(d-n) S_F'(d-n), \quad (69.1) \end{aligned}$$

and

$$\begin{aligned} \langle n | f_p | d \rangle = & (4n_0 d_0)^{-\frac{1}{2}} \\ & \times S_F'(d-n) S_F^{-1}(d-n) \Gamma_d(d-n) u^c(n). \quad (69.2) \end{aligned}$$

These relations will be useful later. Aside from spin dependent factors, the vertex functions $\Gamma_\mu^{(p)}$ and Γ_d are expected to be analytic in the entire complex t plane except for cuts along the real axis for $t \geq (m+\mu)^2$ and $t \geq m^2 + 2\mu(\mu+2\alpha)$, respectively. The propagator S_F' has a pole at $t=m^2$, and a cut along the real axis for $t \geq (m+\mu)^2$. After the spin dependence is extracted, the function $(m^2-t)\Gamma_\mu^{(p)} S_F' \Gamma_d$ is accordingly analytic in the t -plane cut from $t=m^2+2\mu(\mu+2\alpha)$ to $t=\infty$. Its value at the point $t=m^2$ is furthermore known, being just the residue at the proton pole, Eq. (56.2). Assuming proper behavior for $|t| \rightarrow \infty$, we may therefore write a subtracted dispersion relation in t , obtaining symbolically

$$\begin{aligned} \Gamma_\mu^{(p)} S_F' \Gamma_d = & \frac{R_\mu}{m^2-t} - \frac{1}{\pi} \int_{t_0}^{\infty} \frac{\sigma_\mu(t') dt'}{(t'-m^2)(t'-t)}, \\ & t = -(d-n)^2, \quad (70) \end{aligned}$$

where R_μ is given in Eq. (56.2), and σ_μ is the absorptive part of the function $(m^2-t)\Gamma_\mu^{(p)} S_F' \Gamma_d$. This expression has precisely the form expected for the single dispersion relations in the Mandelstam representation for $\langle nd | j_\mu | d \rangle$, namely, a proton pole term plus a single integral.

³¹ H. Lehmann, K. Symanzik, and W. Zimmermann, *Nuovo cimento* **2**, 425 (1955).

It is instructive before considering separately the various factors in Eq. (68) to examine somewhat more closely the representation of this function given in Eq. (70). When the absorptive part of the transition amplitude $\langle np | j_\mu | d \rangle$ is expressed in the usual manner as a sum over intermediate states of bilinear products of matrix elements, the lightest possible intermediate state in the channel in which t is the square of the total energy is that of a single proton, Fig. 12(a). This intermediate state leads to the proton pole term, Eq. (56). The next most massive state involves a pion and a nucleon, Fig. 13(a), and the corresponding contribution to the absorptive part is determined by the matrix elements $\langle p | j_\mu | p' \pi \rangle$ and $\langle p' \pi | f_n | d \rangle$. If these matrix elements are themselves approximated by pole terms, they may be represented by the diagrams shown in Figs. 13(b)(c)(d) and 13(e)(f), respectively. The resultant diagrams obtained from the combinations (bf), (cf), (de), and (df) each contain a single proton as an intermediate state, and contribute to the absorptive part for the single dispersion relation in t . The combinations (bc) and (ce), on the other hand, are not single particle reducible, and contribute only to the Mandelstam double spectral functions. We shall return to these contributions in Sec. IVc. The diagrams (bf) and (cf) evidently represent off-mass-shell corrections to the proton electromagnetic vertex function, while (de) and (df) represent corrections to the neutron-proton-deuteron vertex function and to the proton

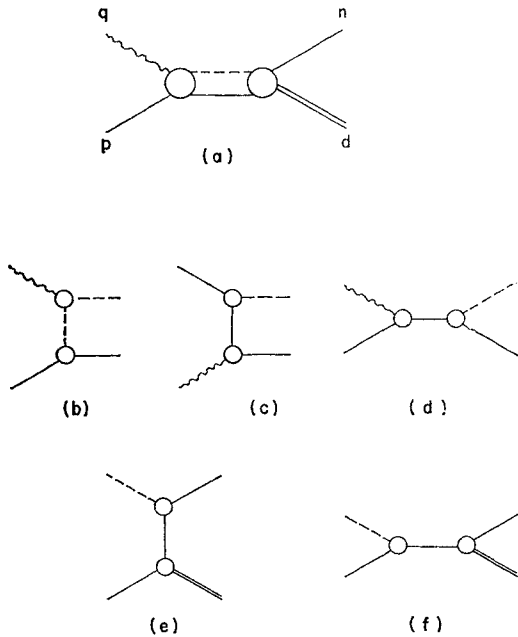


FIG. 13. (a): Diagram for the contribution of the pion-nucleon intermediate state to the absorptive part of $\langle np | j_\mu | d \rangle$. (b), (c), (d): The lowest order diagrams for the matrix element $\langle p | j_\mu | p' \pi \rangle$. (e), (f): The lowest order diagrams for the matrix element $\langle p' \pi | f_n | d \rangle$. The lowest order diagrams for the contribution of the pion-nucleon intermediate state to the absorptive part of $\langle np | j_\mu | d \rangle$ are obtained by combining (b), (c), (d) with (e), (f).

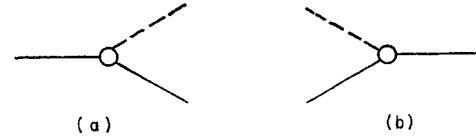


FIG. 14. The lowest order diagrams for the absorptive parts of the matrix elements $\langle n | f_p | d \rangle$ and $\langle p | j_\mu | d - n \rangle$ are obtained by combining respectively diagrams (a) and (b) representing the pion-nucleon vertex function with the sets of diagrams (e), (f), and (b), (c), (d) of Figs. 13.

propagator. This interpretation is easily substantiated. For example, the lowest order contribution to the absorptive part in a dispersion-relation calculation³² of $\Gamma_d(d-n)$ is obtained from Figs. 14(a) and 13(e). It is immediately apparent that this contribution is identical to that obtained for the absorptive part of $\langle np | j_\mu | d \rangle$ from the combination (de) of Figs. 13, except for the presence in the latter of an extra factor containing the proton electromagnetic vertex function on the mass shell and the propagator for the internal proton line. The electromagnetic vertex function depends only on q and does not affect the dispersion integral on t , but the factor $(m^2 - t)^{-1}$ introduced into the integrand by the propagator supplies the extra denominator present in the subtracted form of the dispersion relation given in Eq. (70). The remaining terms in the absorptive part constructed from the diagrams of Figs. 13 have a similar structure, and it is clear overall that the same result could be obtained by calculating directly the lowest order terms in the function σ_μ , Eq. (70), given the absorptive parts of the individual factors in Eq. (68). We therefore turn to an examination of those functions.

Using the relations of Eqs. (69), the result for the single proton contributions to $\langle np | j_\mu | d \rangle$ given in Eq. (68) may be re-expressed in the form

$$\langle np | j_\mu | d \rangle_{\text{single proton}} = \langle p | j_\mu | d - n \rangle S_F(d - n) \times S_F^{-1}(d - n) S_F(d - n) \langle n | f_p | d \rangle. \quad (71)$$

Alternatively, noting that $\langle n | f_p | d \rangle = S_F^{-1}(d - n) \times \langle n | \psi_p | d \rangle$, where ψ_p is the proton field operator, we may write

$$\langle np | j_\mu | d \rangle_{\text{single proton}} = (2p_0)^{-\frac{1}{2}} \bar{u}(p) \times \Gamma_\mu^{(p)}(q, d - n) \langle n | \psi_p | d \rangle. \quad (72)$$

The form given in Eq. (71) is convenient for actual calculations since the untruncated vertex functions $\langle p | j_\mu | d - n \rangle$ and $\langle n | f_p | d \rangle$ are more readily studied using the techniques of dispersion theory than are the truncated functions. On the other hand, the result given in Eq. (72) is particularly simple to interpret. The matrix element $\langle n | \psi_p | d \rangle$ is just the momentum space representation of the wave function of the proton in the deuteron. Thus the matrix element of Eq. (72) is a simple product of the proton electromagnetic

³² R. Blankenbecler and L. F. Cook, Phys. Rev. **119**, 1745 (1960).

vertex function and the proton momentum space wave function, precisely as would be found in the nonrelativistic theory neglecting final-state interactions. We shall return later to this connection.

Blankenbecler and Cook³² have recently made a detailed dispersion theoretic study of the neutron-proton-deuteron vertex function $\langle n|f_p|d\rangle$. The most general form of this function for the proton off the mass shell is given by³²

$$\langle n|f_p|d\rangle = (4n_0d_0)^{-1/2}\{F(t)i\gamma\cdot\xi + G(t)n\cdot\xi + [i\gamma\cdot(d-n) + m][H(t)i\gamma\cdot\xi + I(t)n\cdot\xi]\}u^c(n), \quad (73)$$

where $t = -(d-n)^2$. It is expected on the basis of perturbation theory that the functions F, \dots , will satisfy dispersion relations in t with anomalous thresholds.²⁶ The values of $F(t)$ and $G(t)$ for $t=m^2$ are determined by the neutron-proton effective range and the asymptotic D - to S -state ratio ρ by the relations given in Eqs. (54). It is convenient to utilize this knowledge by writing for $F(t)$ and $G(t)$ dispersion relations subtracted at $t=m^2$. [On the other hand, Blankenbecler and Cook have shown that, if the dispersion relation for $G(t)$ is left unsubtracted, it is possible to calculate ρ , hence, $G(m^2)$, in terms of $F(m^2)$, the deuteron binding energy ϵ , and the pion-nucleon coupling constant.³²] No subtractions are necessary in the dispersion relations for $H(t)$ and $I(t)$. We therefore write

$$F(t) = F(m^2) - \frac{m^2 - t}{\pi} \int_{t_0}^{\infty} \frac{\text{Im}F(t')}{(t' - t)(t' - m^2)} dt', \quad (74.1)$$

$$H(t) = -\frac{1}{\pi} \int_{t_0}^{\infty} \frac{\text{Im}H(t')}{(t' - t)} dt', \quad (74.2)$$

and similar relations for $G(t)$ and $I(t)$. The absorptive part of $\langle n|f_p|d\rangle$ is obtained in the usual fashion by contracting the neutron, and expressing the imaginary part of the resulting expression as a sum over intermediate states. The least massive state is that of a nucleon and a single pion; approximation of the matrix elements $\langle 0|f_p|N\pi\rangle$ and $\langle N\pi|f_n|d\rangle$ in accordance with the graphs of Figs. 13(e) and 14(a) yields, after an analytic continuation necessary to reach the physical sheet,^{32,33} the lowest lying contribution to the absorptive part with the anomalous threshold $t=m^2+2\mu(\mu+2\alpha)$. The next threshold, again anomalous, occurs at $t\approx m^2+4\mu(2\mu+2\alpha)$, and corresponds to a two meson exchange process; this is followed by the normal threshold for the nucleon-single pion intermediate state at $t=(m+\mu)^2$. Although the values of t of physical interest for inelastic electron-deuteron scattering are close to the value $t=m^2$, the lowest anomalous threshold is itself sufficiently close to this value that the contributions to the various functions of the integrals in Eq. (72) are not negligible.

³³ S. Mandelstam, Phys. Rev. Letters 4, 84 (1960).

Recalling that the vertex function $\langle n|f_p|d\rangle$ may be written as $S_F^{-1}(d-n)\langle n|\psi_p|d\rangle$, where the matrix element $\langle n|\psi_p|d\rangle$ represents the wave function of the proton in the deuteron, it is evident that the function $S_F(d-n)\langle n|f_p|d\rangle$ which appears in Eq. (71) should be closely related in an appropriate limit to the nonrelativistic deuteron wave function in momentum space. This connection, already noted in Sec. IVa for the leading terms in $F(t)$ and $G(t)$ [proton pole terms], has been further explored by Blankenbecler and Cook³² and by Bertocchi *et al.*³⁴ Ignoring the spins of the nucleons and the deuteron, those authors show that the nonrelativistic deuteron wave function corresponding to a superposition of Yukawa potentials may be written in momentum space in the form

$$\phi(p)/(4\pi N) = \frac{1}{p^2 + \alpha^2} - \int_{\lambda^2}^{\infty} \frac{\sigma(p'^2)}{p'^2 + p^2} dp'^2, \quad (75)$$

where

$$\int_{\lambda^2}^{\infty} \sigma(p'^2) dp'^2 = 1, \quad (76)$$

p is the center-of-mass 3-momentum of the nucleons, and $\lambda = \mu + \alpha$, with μ the minimum decay constant which appears in the potential. Changing to the variables $t = m^2 - 2(p^2 + \alpha^2)$, $t' = 2p'^2 + m^2 - 2\alpha^2$, it is seen that the function $(p^2 + \alpha^2)\phi(p)$ has precisely the same analytic structure as $F(t)$, Eq. (74.1), with $\sigma(t')$ playing the role of $\text{Im}F(t')/(t' - m^2)$. It may in fact be shown that the function $\text{Im}F(t')/(t' - m^2)$ obtained from the diagrams of Figs. 13(e) and 14(a) is equal in the neighborhood of the anomalous threshold to the function $\sigma(t')$ calculated for a simple Yukawa potential.³² The appearance of $t = -(d-n)^2$ in Eq. (74.1) corresponds to the replacement of p^2 in Eq. (75) by the relativistically corrected value $p^2(1 - p^2/4m^2 \dots)$ which would be obtained in potential theory by including the lowest order relativistic corrections to the Schrödinger equation.

The relation of the functions $F(t), \dots$ to the nonrelativistic deuteron wave function is more complicated in the case of particles with spin. It is convenient in this case to examine the function

$$\bar{u}(p)\langle n|\psi_p|d\rangle = \bar{u}(p)S_F(d-n)\langle n|f_p|d\rangle, \quad (77)$$

in the deuteron rest frame, $\mathbf{p} + \mathbf{n} = 0$, and to neglect relativistic corrections which are of order \mathbf{n}^2/m^2 relative to the leading terms. We then obtain from Eq. (73) for those terms involving $F(t)$ and $H(t)$

$$(4n_0d_0)^{-1/2}\bar{u}(-\mathbf{n}, p_0)S_F(d-n) \times [F(t) + S_F^{-1}(d-n)H(t)]i\gamma\cdot\xi u^c(\mathbf{n}, n_0) \rightarrow -i\sqrt{2}mF(m^2)D(t)\chi_p^*\sigma\cdot\xi\sigma_2\chi_n^{*T}, \quad (78)$$

where

$$D(t) = [F(m^2)]^{-1}[F(t)/(m^2 - t) + H(t)/(2m)]. \quad (79)$$

³⁴ L. Bertocchi, C. Ceolin, and M. Tonin, Nuovo cimento 18, 770 (1960).

The two-component proton and neutron spinors appear in the combination which corresponds to a 3S_1 state, the function $D(t)$ playing the role of the S -state radial wave function in momentum space. According to Eqs. (74), $D(t)$ may be expressed in the form

$$D(t) = \frac{1}{m^2 - t} - \int_{t_0}^{\infty} \frac{\eta(t') dt'}{t' - t}, \quad t_0 = m^2 + 2\mu(\mu + 2\alpha), \quad (80.1)$$

with

$$\eta(t') = [\pi F(m^2)]^{-1} \times [(t' - m^2)^{-1} \text{Im}F(t') - (2m)^{-1} \text{Im}H(t')]. \quad (80.2)$$

Estimates based on the diagrams of Figs. 13(e) and 14(a) indicate that the functions $(t' - m^2)^{-1} \text{Im}F(t')$ and $(2m)^{-1} \text{Im}H(t')$ are comparable in magnitude. A similar reduction of the terms in $\bar{u}(p)\langle n|\psi_p|d\rangle$ which depend on $G(t)$ and $I(t)$ is easily carried through. These terms yield in the non-relativistic limit the D -state component of the deuteron wave function, as well as small corrections to the S -state wave function.

The transition matrix element $\langle np|j_\mu|d\rangle$ may be expressed according to Eq. (72) in terms of the vertex function $\langle n|\psi_p|d\rangle$. Since the cross section $d^2\sigma/(d\Omega_e dE_e')$ depends in the neighborhood of the quasi-elastic peak primarily on the low-momentum components of this function, the spin dependence of the matrix element may be approximated as discussed in Sec. IVa. The resulting form of $\langle np|j_\mu|d\rangle$ involves the invariant functions $F(t)$, . . . , only in the combination $D(t)$ and a similar combination which corresponds to the deuteron D -state wave function. It is found in the nonrelativistic theory that the use of the asymptotic form of the deuteron wave function $u(r)$ instead of the complete function in the calculation of the peak value of the cross-section $d^2\sigma/(d\Omega_e dE_e')$ changes this quantity by roughly 16% for the values of the electron momentum transfer of current interest. Use of the asymptotic wave function is equivalent to retaining only the nucleon pole terms in $\langle np|j_\mu|d\rangle$ (see Sec. IVa). The short-range structure of the deuteron wave function is given in the nonrelativistic theory by the integral in Eq. (75), and, as we have seen, by the integral in Eq. (80) in the relativistic theory. It is therefore evident that the functions $[F(t) - F(m^2)]$, $H(t)$, . . . , need not be known with great accuracy in order to obtain an accurate peak value of $d^2\sigma/(d\Omega_e dE_e')$. There are several possibilities with regard to these functions. The most sophisticated approach would involve a fundamental calculation of the absorptive parts $\text{Im}F(t)$, However, this does not appear to be necessary for those values of t which are of interest; the integrals depend most strongly on the values of the absorptive parts in the anomalous region, where they may be identified with the nonrelativistic weight functions $\sigma(t')$. For example, the Hulthén wave function used in the calculations of Secs. II and III corresponds to the use in Eq. (75) of a

weight function

$$\sigma(p'^2) = \delta(p'^2 - \beta^2) \rightarrow \delta(t' - \nu^2), \\ \nu^2 = m^2 + 2(\beta^2 - \alpha^2).$$

For the usual parameter $\beta = 1.434 \text{ f}^{-1}$, the singularity lies in the anomalous region just below the two pion threshold $t = m^2 + 4\mu(2\mu + 2\alpha)$. The use of the corresponding weight function $\eta(t') = \delta(t' - \nu^2)$ in Eq. (80) leads to a covariant generalization of the Hulthén model,³² but may be regarded alternatively as the approximation of the entire spectral function for $t \geq m^2 + 2\mu(\mu + 2\alpha)$ by a single pole. More realistic models may of course be obtained using weight functions calculated from a specific two-nucleon interaction. Another reasonable procedure in the present case would be the direct calculation of $\text{Im}F(t')$, . . . , in the lowest anomalous region, and the replacement of the remainder of the cuts by poles. The positions and residues of the poles may be fixed by requiring that the wave function vanish for $t \rightarrow -\infty$, and that it reproduce correctly the deuteron effective range and quadrupole moment.³⁵ The differences in the peak values of $d^2\sigma/(d\Omega_e dE_e')$ associated with different models for the short range structure of the deuteron wave function are in any case small; such a drastic change as from a Hulthén model to the hard core model given in Sec. III changes the peak value of the cross section by only 1.3%.

It is clear that the foregoing discussion applies equally well to the contributions to the transition amplitude $\langle np|j_\mu|d\rangle$ of the single dispersion relation in $u = -(d-p)^2$, and a similar type of discussion is easily carried through for the dispersion relation $s = -(d+q)^2$. The latter, which affects only transitions to final 3S_1 and 3D_1 states for the nucleons, is not important for momenta in the region of the quasi-elastic peak but is dominant near the threshold for deuteron breakup. A careful consideration of this dispersion integral is therefore essential to the relativistic generalization of the discussion of Sec. III, but will not be undertaken in the present paper.

This section will be concluded with a brief discussion of the truncated proton vertex function $\Gamma_\mu^{(p)}(d-n)$ which appears in Eq. (72). For the present purposes, we are less interested in calculating this function than in estimating the difference between its values for the internal proton on and off the mass shell; the on-shell value depends only on the measurable proton form factors as defined in Eq. (51). [Were we considering instead the single neutron contributions to the transition amplitude $\langle np|j_\mu|d\rangle$, the on-shell value of the corresponding vertex function $\Gamma_\mu^{(n)}$ would depend only on the neutron form factors which are to be determined

³⁵ It may be remarked that the repulsive core deuteron wave function used in Sec. III corresponds to a set of poles with fixed residues; the parameter μ determined the location of all poles simultaneously. A more flexible model may be obtained by adjusting independently the location and residue of each pole.

from the electron-deuteron scattering experiments.] On the basis of the singularities found in perturbation theory, it is expected that, when $\Gamma_\mu^{(p)}$ is resolved into an appropriate set of spin-dependent factors multiplied by invariant functions, the latter will satisfy dispersion relations in the variable $t = -(d-n)^2$. The known values of the invariant functions for $t=m^2$ may be utilized to make a subtraction in the dispersion relations, these then being of the form

$$\Gamma(t) = \Gamma(m^2) - \frac{(m^2-t)}{\pi} \int_{(m+\mu)^2}^{\infty} \frac{\text{Im}\Gamma(t')}{(t'-t)(t'-m^2)} dt'. \quad (81)$$

The threshold at $t=(m+\mu)^2$ corresponds to the least massive intermediate state which can contribute to $\text{Im}\Gamma(t')$, that of a nucleon and a single pion. The lowest order diagrams for the absorptive part are obtained by combining Figs. 13(b),(c) with Fig. 14(b). Because of the subtraction, the integral in Eq. (81) should converge rapidly, and it may in fact be reasonable to estimate its value using only these diagrams. However, the requisite analysis will be deferred to a future paper. We will confine our present remarks to the observation that it is plausible from the form of Eq. (81) that the off-mass-shell corrections to $\Gamma(t)$ will be on the order of $-(m^2-t)/(2m\mu)$ relative to $\Gamma(t)$ itself for $t \approx m^2$. The average value of (m^2-t) is roughly $6m\epsilon$ at the quasi-elastic peak in the cross-section $d^2\sigma/(d\Omega_d dE_e')$ for any reasonable model of the deuteron and values of q in the range of present interest. Thus, one might expect individual functions $\Gamma(t)$ to differ from their values on the mass shell by about $-3\epsilon/\mu \approx -5\%$, but this is probably an overestimate. The over-all effect on the cross section $d^2\sigma/(d\Omega_d dE_e')$ is less evident. Careful study of this effect is obviously required. We remark finally that an alternative approach to the study of the truncated vertex function $\Gamma_\mu^{(p)}$ is afforded by the identity given in Eq. (69.1). The structure of the complete proton vertex function $\langle p | j_\mu | d-n \rangle$ which appears there was examined by Bincer,³⁶ who proved rigorously that it satisfies dispersion relations in the variables t and \sqrt{t} . The modified proton propagator $S_F'(d-n)$ is known also to satisfy dispersion relations in t .³⁷ One could therefore hope in principle to obtain the off-mass-shell corrections to $\Gamma_\mu^{(p)}$ by computing separately the corrections to $\langle p | j_\mu | d-n \rangle$ and $S_F'(d-n)$. However, calculation of the absorptive parts for the dispersion relations is itself a formidable task, even for the pion-nucleon intermediate state, and a diagrammatic analysis is simpler for the function $\Gamma_\mu^{(p)}$ itself.

c. Double Dispersion Relations

We turn finally to a brief discussion of the double spectral functions which enter the Mandelstam repre-

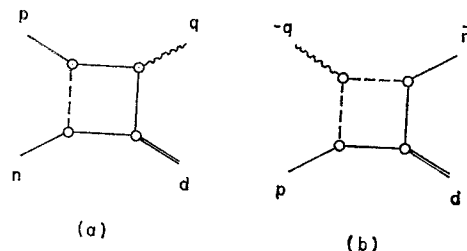


FIG. 15. The lowest order diagrams which give contributions to the double spectral functions in s and t (a), and t and u (b), in the Mandelstam representation for the transition amplitude $\langle np | j_\mu | d \rangle$.

sentation for the transition matrix element $\langle np | j_\mu | d \rangle$. The lowest order diagram which contributes to the spectral function in s and t is shown in Fig. 15(a); a similar diagram with the neutron and proton interchanged gives the lowest order contribution in s and u . These diagrams represent a modification of the transition amplitude by interactions between the outgoing nucleons. It is easily verified that both diagrams lead to normal thresholds in s at $s=4m^2$. However, the thresholds in t and u occur at the anomalous values²⁶ $(t,u)=m^2+2\mu(\mu+2\alpha)$ encountered previously in the discussion of the single dispersion relations in those variables; higher anomalous thresholds are also present. The occurrence of the anomalous thresholds is again indicative of the composite structure of the deuteron. One may accordingly expect the double spectral functions to be closely related in the anomalous regions to the nonrelativistic wave functions for the neutron-proton system. DeAlfaro and Rossetti have made a partial investigation of this connection for the case of deuteron photodisintegration ($q^2=0$),³⁸ demonstrating in particular that the singularities of the partial wave transition amplitudes as functions of s and (t,u) deduced from a potential model with spinless nucleons interacting through a Yukawa potential, coincide with those displayed by the Mandelstam representation with the indicated anomalous thresholds. Although this work was somewhat incomplete from the present point of view, since the precise connection between the double spectral functions and the nonrelativistic wave functions was not determined, it is clear that such a connection exists.

The foregoing results are immediately applicable in the present case, $q^2>0$. The values of t and u of primary interest in the calculation of the peak value of the cross section $d^2\sigma/(d\Omega_d dE_e')$ are close to the value m^2 , hence, to the anomalous thresholds in those variables. One may therefore expect the main contributions to $\langle np | j_\mu | d \rangle$ from the double dispersion relations to arise from the anomalous regions, $m^2+2\mu(\mu+2\alpha) \leq (t,u) \leq (m+\mu)^2$, thus, to be describable using nonrelativistic wave functions for the initial and final states of the two-

³⁶ A. M. Bincer, Phys. Rev. **118**, 855 (1960).

³⁷ G. Källén, Helv. Phys. Acta **25**, 417 (1952). H. Lehmann, Nuovo cimento **11**, 342 (1954).

³⁸ V. DeAlfaro and C. Rossetti, Nuovo cimento **18**, 783 (1959). A. Martin, *ibid.* **19**, 344 (1961).

nucleon system. Examination of the results of DeAlfaro and Rossetti³⁸ then indicates that the matrix elements K_{JLS} defined in Eq. (13) will be correct relativistically at the quasi-elastic peak if the q which appears in the definition is interpreted as the magnitude of the electron 3-momentum transfer in the center-of-mass system of the outgoing nucleons; as noted previously, this is equal at the peak to $(q^2)^{1/2}$. Wave function calculations of the type discussed in Secs. I and II should therefore be fairly reliable. It may nevertheless be advantageous in some respects to use an alternative procedure. It is probable that soluble integral equations of the Omnès type³⁹ can be derived for the partial wave transition amplitudes using the fact that the amplitude leading to a given final state of the two-nucleon system has the phase characteristic of neutron-proton scattering in that state, at least up to $s = (2m + \mu)^2$. If this is the case, the changes in the partial wave amplitudes caused by final state interactions can be expressed in terms of integrals involving the experimentally determined scattering phase shifts. We hope to investigate this procedure in more detail in the future.

The lowest order term in the double spectral function in t and u is obtained from the diagram of Fig. 15(b), which represents a contribution to the transition current operator associated with meson exchange currents. This is perhaps the most interesting of those contributions to $\langle n\mathbf{p} | j_\mu | d \rangle$ which have yet to be calculated, but the effect on the peak cross section is difficult to estimate. We note only that configurations in which the nucleons are sufficiently close together that exchange of a meson is likely, yield only a relatively small fraction of the cross section $d^2\sigma/(d\Omega_e dE_e')$. This suggests that exchange current effects may not be too important. The same conclusion may be drawn from the dispersion relation, if it is assumed, as seems probable, that the double spectral function is large only for t and u simultaneously close to the anomalous thresholds, say $m^2 + 2\mu(\mu + 2\alpha) \leq (t, u) \leq (m + \mu)^2$. The physical values of t and u are given in the center-of-mass system for the outgoing nucleons, $\mathbf{p} + \mathbf{n} = 0$, by

$$t = m^2 - 2[\alpha^2 + p^2 + \frac{1}{4}q^2 - \mathbf{p} \cdot \mathbf{q}],$$

$$u = m^2 - 2[\alpha^2 + p^2 + \frac{1}{4}q^2 + \mathbf{p} \cdot \mathbf{q}].$$

Since $p = \frac{1}{2}q = |\frac{1}{2}\mathbf{q}|$ at the quasi-elastic peak in $d^2\sigma/(d\Omega_e dE_e')$ the double dispersion integral is weighted toward large values of at least one of the variables, and the corresponding contribution to the transition amplitude may reasonably be expected to be small. The author hopes to make a detailed study of this matter in the near future.

We remark finally that the situation is much more complicated with respect to the calculations given in Sec. III; the values of t and u of importance near the threshold for deuteron breakup differ sufficiently from the value m^2 that contributions to both the single and

the double dispersion integrals from nonanomalous regions in the spectral functions may be important. Furthermore, the nucleons are on the average considerably off the mass shell, and the use of free-particle form factors in the nucleon electromagnetic vertex functions is unlikely to be a good approximation. The results of Sec. III based on a wave function type of analysis and free-particle form factors are accordingly less well grounded theoretically than those of the preceding sections.

d. Summary of Sec. IV

The present section has been devoted to the study of the main features of a dispersion-theoretic calculation of the cross section $d^2\sigma/(d\Omega_e dE_e')$ for inelastic electron-deuteron scattering. The principal emphasis has been on those conditions which prevail in the neighborhood of the quasi-elastic peak, but the discussion may readily be broadened to include other situations as well. The transition amplitude $\langle n\mathbf{p} | j_\mu | d \rangle$ was assumed to satisfy a Mandelstam representation, with single dispersion relations and pole terms in each of the variables $s = -(d + q)^2$, $t = -(d - n)^2$, and $u = -(d - p)^2$, and double dispersion relations in the three pairs of variables. The dominant contributions to $\langle n\mathbf{p} | j_\mu | d \rangle$ in the region of the quasi-elastic peak arise from the pole terms and single dispersion relations in t and u . The pole terms were shown in Sec. IVa to reproduce with some relativistic modifications the transition matrix element which would be obtained in the nonrelativistic theory by approximating the deuteron wave function by its asymptotic form; the nucleon form factors for the nucleons on the mass shell appear in the resulting expressions. Modifications of these simple results connected with the single dispersion relations in t and u were studied in Sec. IVb. The thresholds in the dispersion relations were in each case anomalous, but the spectral functions in the anomalous regions were found to be closely related to the nonrelativistic deuteron wave function. This relationship, and the relative insensitivity of the peak cross section to the short-range structure of the deuteron wave function, permit a reliable, albeit approximate, evaluation of the spectral functions in the region in which they are needed. Inclusion of the single dispersion relations results also in the modification of the nucleon form factors for the effects of binding. However, rough estimates indicate that the differences between the free-nucleon form factors which appear in Eq. (56) (and its analog for the neutron pole term) and the form factors for a nucleon off the mass shell which appear in Eq. (72), are quite small, probably on the order of the ratio $\epsilon/\mu \approx 1.6\%$. Section IVc was devoted to the discussion of the double dispersion relations. These express, among other effects, the modification of the transition amplitude by interactions between the outgoing nucleons. However, anomalous thresholds are again present, and it is evident on the basis of the

³⁹ R. Omnès, Nuovo cimento 8, 316 (1958).

work of DeAlfaro and Rossetti,³⁸ that a wave function analysis of the effects of final-state interactions on the scattering should be valid in the neighborhood of the quasi-elastic peak. The contribution to the scattering of meson exchange currents is also given by the double dispersion relations, but this effect has yet to be evaluated.

Calculations of the cross-section $d^2\sigma/(d\Omega_e dE_e')$ for inelastic electron-deuteron scattering have been carried out using the approximate form of the transition amplitude

$$\langle n p | j_\mu | d \rangle \approx e(8p_0 m_0 d_0)^{-1} [D(t) J_\mu^p + D(u) J_\mu^n], \quad (82)$$

where $D(t)$ is the relativistic S -state wave function for the deuteron defined in Eqs. (79) and (80). The spin-dependent factors J_μ^p and J_μ^n were used in the approximation of Eq. (62) and the contribution to the scattering of the D -state component of the deuteron wave function was neglected. The results of this calculation are given formally in Eqs. (10), (11), and (15). The functions $M(p, q)$ and $N(p, q)$ which correspond to the covariant Hulthén model for $D(t)$ are given in Eqs. (28)–(30). The parameters x and y which enter these functions should strictly be written as

$$x = [\alpha^2 + p^2 + \frac{1}{4}q^2] p^{-1} |\mathbf{q}|^{-1} \quad (83.1)$$

and

$$y = [\beta^2 + p^2 + \frac{1}{4}q^2] p^{-1} |\mathbf{q}|^{-1}, \quad (80.4)$$

where q^2 is the square of the electron 4-momentum transfer, while \mathbf{q} is the 3-momentum transfer in the center-of-mass system of the outgoing nucleons. The definitions of x and y given in Eq. (28) are correct at the quasi-elastic peak, but are only approximate elsewhere. The values of $M(p, q)$ and $N(p, q)$ arising from more refined wave functions of the type indicated in Eq. (80) are easily derived using the methods outlined in the Appendix. The results given in Eqs. (10), (11), and (15) neglect: (1) the effect of final-state interactions between the nucleons, (2) the effects of meson exchange currents, and (3) off-mass-shell corrections to the nucleon form factors; and are of course approximate in the treatment of the deuteron wave function. They nevertheless constitute an excellent approximation to the exact cross section in the region of the quasi-elastic peak. We would like to call particular attention to the kinematic factor (m/E) which enters the cross section as given in Eq. (10). This factor, which arises from the calculation of the final three-body phase space, would reduce to unity in the nonrelativistic theory. It was included in the results given in the Appendix to (I),⁹ but has apparently been neglected thus far in those analyses of the experimental data based on the modified Jankus cross section.^{4,40,41} Since $p = \frac{1}{2}q$ at the peak, the factor (m/E) reduces the peak cross section by $[1 + q^2/(4m^2)]^{-1}$, a factor equal to 0.95, 0.92, 0.88, and

0.85 for $q = 3, 4, 5, 6 \text{ f}^{-1}$. The correct factor appears in the results obtained by Goldberg⁴¹ from a calculation based on the impulse approximation. It should in addition be remarked that the factor which multiplies $M(p, q)$ in Eq. (15.1) is given incorrectly by the modified Jankus theory, as was pointed out in (I).⁹ These changes account for the discrepancy between the values of the peak cross section calculated using Eqs. (10), (15), and (31), and the results obtained from the modified Jankus theory by Herman and Hofstadter,⁴⁰ and lead to important differences between the values of the neutron form factors obtained using the two theories. This will be discussed in detail in the next section.

V. DISCUSSION

We wish in the present section to summarize the main results of this paper, and to review briefly the status of the theory of inelastic electron-deuteron scattering. We have been concerned primarily with the influence on the cross section $d^2\sigma/(d\Omega_e dE_e')$ of the interactions between the outgoing nucleons, and with the relation of the relativistic to the non-relativistic theories of the scattering. We will consider first the results obtained for final electron energies in the region of the large peak which corresponds to quasi-elastic scattering of the electron from a single nucleon. The dominant terms in the transition amplitude $\langle n p | j_\mu | d \rangle$ for the neutron-proton system arise in the relativistic theory from nucleon pole terms and single dispersion relations which appear in a Mandelstam representation for this quantity. The pole terms are completely specified by the known asymptotic normalization of the deuteron wave function and the electromagnetic form factors for free nucleons. This fact is basic to the Chew-Low type of extrapolation procedure suggested by Bose²⁹ for the determination of the neutron magnetic form factor. The single dispersion relations correct the pole terms by taking into account the short-range structure of the deuteron wave function, and effects on the nucleon electromagnetic vertex functions associated with the binding of the particles. The latter effects are probably quite small. The cross section is rather insensitive to the short-range structure of the wave function; transition from a Hulthén to a more realistic repulsive-core wave function leads only to a 1.3% increase in the peak value. It is therefore possible to reformulate the theory in terms of the nonrelativistic deuteron wave function as discussed in Sec. IV without incurring any serious errors. The resulting theory differs from the semi-relativistic approximation discussed in (I) only in minor details. However, it establishes clearly for the first time the proper dependence of the transition matrix element on the various kinematical quantities, and the limits within which it is possible to analyze the cross section $d^2\sigma/(d\Omega_e dE_e')$ in terms of a deuteron wave function and free-nucleon form factors. The effects on the peak cross section of interactions between the outgoing nucleons were considered in the semirelativistic approximation.

⁴⁰ R. Herman and R. Hofstadter, *High-Energy Electron Scattering Tables* (Stanford University Press, Stanford, California, 1960).

⁴¹ A. Goldberg, *Phys. Rev.* **112**, 618 (1958).

The changes in individual partial wave matrix elements calculated using approximate wave functions matched to the experimentally determined phase shifts were found to be quite large. The over-all change in the peak cross section was nevertheless small, probably fortuitously, for the two situations considered, $p = \frac{1}{2}q = 1.3, 1.7 \text{ f}^{-1}$. The situation has not been studied in detail for the much larger values of q which are now of interest, but it appears improbable that the changes in the peak cross section caused by final state interactions will become large.

We have thus far ignored entirely the effect on the scattering of the D -state component of the deuteron wave function. This was treated formally in Appendix II of (I),⁹ and estimates of the over-all corrections to the cross section were made at that time. The results of a more detailed examination of the errors in the peak cross section incurred for $p = \frac{1}{2}q = 1.3 \text{ f}^{-1}$ by using a pure S -state wave function are summarized in Table IV. The calculations were based on a Hulthén-type wave function with a 5% D -state probability.^{9,18} It is evident from Table V that the D -state component of the wave function scatters much less efficiently than the S -state component. Thus, the pure D -state scattering is only 1.6% of the S -state scattering, despite the 5% D -state probability. The over-all effect is further reduced by interference terms involving both the S - and D -state wave functions, the contribution to the cross section of all terms involving the D -state component amounting to only 0.72% of the total. Since the S -state component of the wave function is now normalized to 0.95 instead of unity, the peak cross section calculated with the complete wave function is 4.3% smaller than that calculated using the same S -state wave function, but normalized to unity. It should be noted, however, that the S -state component of the complete wave function is not matched to the neutron-proton effective range, as was assumed in the preceding sections; both the S - and D -state components enter the calculation of that quantity.¹⁸ If the peak cross section calculated for the complete wave function is compared to that calculated for an S -state wave function matched to the effective range, the 4.3% discrepancy noted above is reduced to 2.9%. Scattering involving the D -state component of the wave function should become somewhat more important at larger values of the momentum transfer q .

Combining the foregoing results, we obtain as a "best" result for the peak cross section for the range of momentum transfers of current interest

$$d^2\sigma/(d\Omega_e dE_e') = \sigma_{\text{Mott}}(4.57 \times 10^{-3}) \times (1 \pm 0.05)(m^2/pE)(G_p + G_n), \quad p = \frac{1}{2}q, \quad (84)$$

where

$$G_i = F_{1i}^2 + (q^2/4m^2)\kappa_i^2 F_{2i}^2 + 2(q^2/4m^2) \tan^2(\frac{1}{2}\theta)(F_{1i} + \kappa_i F_{2i})^2. \quad (85)$$

This approximate result is based on the expression of

TABLE V. The relative contributions of various terms to the cross section $d^2\sigma/(d\Omega_e dE_e')$, calculated for $p = \frac{1}{2}q = 1.3 \text{ f}^{-1}$ and a Hulthén-type model for the deuteron wave function. The D -state probability for this wave function is 5%. It was assumed in the calculations that $F_{1p} \approx F_{2p} \approx F_{2n}$ and $F_{1n} \approx 0$. The labeling according to S and D states refers to the part of the wave function which contributes to each term. The auxiliary designations pp , nn , and np refer to terms in the cross section which arise, respectively, from scattering by the proton alone, by the neutron alone, and from interference between the neutron and proton scattering amplitudes.

Terms in cross section	Relative contribution
S -state, pp plus nn	1.00
S -state, np interference	-0.21×10^{-2}
D -state, pp plus nn	1.56×10^{-2}
S - D , np interference	-0.87×10^{-2}
D -state, np interference	0.03×10^{-2}
Total	$1 + 0.51 \times 10^{-2}$

Eqs. (10), (11), and (15). The function $M(p, q)$ was evaluated for $p = \frac{1}{2}q$ and the repulsive-core deuteron wave function of Sec. II using the method discussed in the Appendix. The following corrections to the cross section were then incorporated in the result: (1), a -3% correction arising from the neglect of the D -state component of the deuteron wave function; (2), a -2% correction for the effects of final state interactions. The latter is strictly valid only for the range of momentum considered in Sec. II, $2.6 \text{ f}^{-1} < q < 3.4 \text{ f}^{-1}$, but is probably a reasonable estimate of the effects of final state interactions for somewhat larger values of q as well. The deuteron normalization constant N^2 which appears in $M(p, q)$ was evaluated using for the triplet effective range the value $r_{0,T} = 1.69 \pm 0.03 \text{ f}$ appropriate for the small positive shape-dependent parameter $P_T = 0.03$ which seems necessary to fit the low-energy neutron-proton scattering data.¹⁸ The indicated uncertainty in the result encompasses the experimental uncertainty in $r_{0,T}$, an estimated 2% uncertainty in the cross section associated with final-state interactions, and a possible 1% error associated with uncertainties in the deuteron wave function and with the D -state scattering. Negligible errors were introduced by neglecting the interference terms in Eq. (15). We have also neglected in the calculations contributions to the transition matrix element which arise from the nonzero momentum of the spectator particle in the spin-dependent factor J_μ , [Eqs. (56.2) and (62)]; the error incurred thereby is again negligible at the quasi-elastic peak.

The modifications the peak cross section which arise from off-mass-shell corrections to the nucleon form factors and, more important, from scattering by meson currents within the deuteron, have not yet been calculated, but the changes are probably no more than a few percent of the peak value. The cross section is also modified to some extent by radiative corrections to the electron current operator and the photon propagator, and by the emission of bremsstrahlung in the course of the scattering. These corrections have been discussed

elsewhere.^{42,43} We remark only that, to the extent to which radiation by the nucleons can be neglected, these corrections alter only the external factor in Eq. (84), and do not affect the functions G_p and G_n .

The form for the peak cross section given in Eq. (84) is identical to that given by Goldberg⁴¹ in an approximation to his impulse type calculations; the relation of the function $M(p, q)$ for $p = \frac{1}{2}q$ to Goldberg's matrix element $\langle 1/p \rangle$ is discussed in the Appendix. However, the present approach allows an unambiguous study of the approximations leading to Eq. (85). The result appears, in fact, to be more accurate than was supposed by Goldberg.

Most analyses of the inelastic electron-deuteron scattering experiments⁴ have been based on the modified Jankus cross section.⁴⁰ The factor O^2 which appears in that result may be considerably simplified at the quasi-elastic peak if the very small terms arising from the contribution of nonzero initial momenta of the target nucleon to the nucleon convection current, and from interference scattering involving both the neutron and the proton, are omitted. The resulting function may be expressed in terms of $M(p, q)$ [Eq. (29)]. When $M(p, q)$ is treated as in Eq. (31), the resulting peak cross section differs from that given in Eq. (84) in the following respects. First, the kinematic factor (m/E) and the corrections for D -state effects and final state interactions which have been incorporated in Eq. (84) are absent. Second, the functions G_p and G_n are replaced by functions G_p' and G_n' given by

$$G_i' = G_i - (q^2/2m^2)F_{1i}^2 - O[(q^2/4m^2)^2].$$

This change is quite important for small scattering angles and large values of q^2 . The origin of the extra terms is easily traced. Those terms involving $(q^2/4m^2)^2$, which cannot consistently be retained in the non-relativistic theory [see reference 9], represent partial corrections which lead to the appearance of the 4-momentum transfer rather than the 3-momentum transfer in the relativistic theory. These terms should be omitted. The extra (and more important) term $-(q^2/2m^2)F_{1i}^2$ should also be omitted. The transition from the Jankus⁸ to the modified Jankus cross section⁴⁰ may be accomplished essentially by replacing the effective charge eF_{1i} in the non-relativistic interaction Hamiltonian by $e[F_{1i} - (q^2/4m^2)(F_{1i} + 2\kappa_i F_{2i})]$. As noted in reference 30, the correct effective charge is

$e[F_{1i} - (q^2/4m^2)(-F_{1i} + 2\kappa_i F_{2i})]$. However, the first form leads to results correct to $O(m^{-2})$ if one simultaneously omits the convection current terms in the interaction.^{9,30} These were incorrectly included in the modified Jankus cross section. [The extra terms were correctly omitted in (I).⁹]

The possible effect of the foregoing results on the values of the neutron form factors F_{1n} and F_{2n} determined from the Stanford electron scattering experiments, has been investigated by reanalyzing the experimental data of Hofstadter, deVries, and Herman^{4,44} for representative values of q^2 . The calculations were based on the theoretical expression for the peak value of the inelastic deuteron cross section $d^2\sigma/(d\Omega_e dE_e')$ given in Eq. (84). The function G_p which appears there was evaluated using the Rosenbluth cross section for elastic electron-proton scattering,

$$(d\sigma/d\Omega_e)_p = \sigma_{\text{Mott}}[1 + (2E_e/m) \sin^2(\frac{1}{2}\theta)]^{-1} G_p \quad (86)$$

in conjunction with experimental values of the elastic scattering cross sections.² The value of the Rosenbluth factor G_n for the neutron was then determined from the experimental deuteron cross section using Eq. (84). Where properly matched values of $d^2\sigma/(d\Omega_e dE_e')$ and $(d\sigma/d\Omega_e)_p$ were not available in the published data, we have constructed "experimental" cross sections using the modified Jankus theory and the smoothed values of the form factors taken from Fig. 1 of reference 4.⁴⁵ A corrected value of G_n was then determined using the cross section of Eq. (84). Separate values of F_{1n} and F_{2n} were obtained by combining values of G_n obtained at a fixed value of q^2 , but with different scattering angles and energies, using the method of intersecting ellipses.⁴⁰ We note finally that the ellipses failed in three cases [$q^2 = 10, 11.5$, and 15 f^{-2}] to intersect unless allowance was made for possible errors in the cross sections.⁴⁶ In

⁴⁴ The author is greatly indebted to Professor R. Hofstadter, Dr. C. deVries, and Dr. R. Herman for extensive discussions concerning the Stanford electron scattering experiments.

⁴⁵ For $q^2 = 11.5, 18.0$, and 21.0 f^{-2} , we have used the experimental peak values of $d^2\sigma/(d\Omega_e dE_e')$ given by Hofstadter, deVries, and Herman^{4,44} in conjunction with the experimental proton cross sections $(d\sigma/d\Omega_e)_p$ for the same scattering angles and energies given by Hofstadter, Bumiller, and Croissiaux.² For $q^2 = 5.1 \text{ f}^{-2}$, the values of $d^2\sigma/(d\Omega_e dE_e')$ interpolated from the data of Sobottka⁴ by Hofstadter, deVries, and Herman⁴ were combined with proton cross sections calculated from the exponential proton model of Chambers and Hofstadter.¹ This model was used by Sobottka to normalize his deuteron cross sections.⁴ The deuteron cross sections used in the analysis for $q^2 = 10 \text{ f}^{-2}$ and 15 f^{-2} were calculated from the modified Jankus cross section⁴⁰ using smoothed values of the nucleon form factors taken from Fig. 1 of Hofstadter and Herman.⁴ The values assumed for the neutron form factors F_{1n} and F_{2n} corresponding to the Jankus theory are given in Table VI. The values assumed for the proton form factors are as follows: $q^2 = 10 \text{ f}^{-2}$, $F_{1p} = 0.48$, $F_{2p} = 0.39$; $q^2 = 15 \text{ f}^{-2}$, $F_{1p} = 0.43$, $F_{2p} = 0.21$.

⁴⁶ The failure of the ellipses to intersect indicates that the input data are inconsistent with the theoretical cross section of Eq. (84). However, intersections could be obtained by changing either the large angle or the small angle deuteron cross section $d^2\sigma/(d\Omega_e dE_e')$ by 10% or less. Errors in the cross sections of this magnitude are consistent with the estimated accuracy of the experiments.^{2,4} Furthermore, such errors are undoubtedly present, as indicated by the deviation of the experimental values of G_n from the values

⁴² S. Sobottka, Phys. Rev. **118**, 831 (1960).

⁴³ Y. S. Tsai, Phys. Rev. **122**, 1898 (1961). Tsai gives detailed numerical examples for the conditions of the Stanford electron-proton scattering experiments, which indicate that radiative corrections involving the proton will become important for large-angle scattering at energies E_e near 1 Bev. However, corresponding corrections for the neutron will be absent to the accuracy to which the calculations were performed. The radiative corrections are associated primarily with bremsstrahlung and the exchange of virtual photons with low momenta; in either case, the vanishing of F_{1n} for $q^2 = 0$ causes the relevant portions of the matrix elements to vanish also. The magnetic moments do not contribute significantly to the radiative corrections.

these cases, we have determined rough values of F_{1n} and F_{2n} by choosing as the "intersection" the midpoint of the region of closest approach. It is expected from an examination of the effects of possible experimental errors that the value of F_{2n} so determined is slightly too small, and that of F_{1n} , considerably too negative. $F_{1n} \approx 0$ would be consistent with the data within the possible errors.

The results of this analysis are quite striking, as may be seen from Table VI. The original results of Hofstadter *et al.*,⁴ based on the modified Jankus cross section, suggested that F_{1n} was a positive increasing function of q^2 , with a value $F_{1n} \approx 0.2$ for $q^2 = 20 \text{ f}^{-2}$. Preliminary results obtained using the present theory favor very small or zero values of F_{1n} over the entire range of q^2 which was considered. In addition, the new values of F_{2n} are somewhat smaller than those based on the Jankus theory, bringing this form factor more nearly into coincidence with F_{2p} . However, these conclusions must be regarded as tentative pending a complete analysis of more recent Stanford and Cornell data.⁴⁷

The theoretical situation is much less clear with respect to the cross-section $d^2\sigma/(d\Omega_e dE_e')$ near the threshold for the dissociation of the deuteron. For large values of q , the cross section depends critically on the structure of the deuteron and the free 3S_1 and 1S_0 neutron-proton wave functions at small distances. The nucleons are then considerably off the mass shell, and it is not clear either that the effective form factors do not differ significantly from the free-nucleon form factors, or that the effects on the scattering of meson exchange currents are negligible. It does not, therefore, appear likely that reliable information about the structure of the nucleons can be obtained from experiments of the type performed by Kendall *et al.*¹⁰ (This statement is equally true of the elastic electron-deuteron scattering experiments of McIntyre and his co-workers.⁶) The purely phenomenological analysis of Sec. III may nevertheless have some merit as a check on the possible short-range structure of the free-state

calculated for the same q^2 and θ using neutron form factors taken from smooth curves drawn through the points by Hofstadter and Herman.⁴ The deviations range up to 50% but are generally much smaller. Since scattering by the proton contributes $\frac{1}{3}$ – $\frac{2}{3}$ of the peak deuteron cross section, depending on q^2 and θ , the corresponding errors in $d^2\sigma/(d\Omega_e dE_e')$ are reduced by factors of 2–3, and lie within the expected range. Conversely, it is clear that the values obtained for G_n , hence, for the neutron form factors, can be changed significantly by rather small changes in the experimental values of $d^2\sigma/(d\Omega_e dE_e')$ and $(d\sigma/d\Omega_e)_p$.

⁴⁷ The Stanford group has recently extended its measurements of the inelastic electron-deuteron, and the elastic electron-proton, scattering cross sections to a number of energies and scattering angles not previously considered, with a largest value of q^2 now 25 f^{-2} . Preliminary analyses at several of the new points suggest that F_{1n} may indeed be greater than zero, but somewhat smaller in magnitude than indicated in reference 4. [R. Hofstadter (private communication). The author is greatly indebted to Professor Hofstadter for a number of communications concerning the Stanford experiments.] The Cornell group has also extended considerably its measurements at larger values of q^2 . [R. R. Wilson (private communication).]

TABLE VI. Changes in the neutron form factors F_{1n} and F_{2n} which result from changes in the theoretical peak value of $d^2\sigma/(d\Omega_e dE_e')$. The form factors with the superscript J result from an analysis of the experimental cross sections^a based on the modified Jankus theory.^b The form factors without superscripts are obtained when the data are reanalyzed using the present theory. The calculations were based on the method of intersecting ellipses.^b The tabulated values of the form factors denoted by asterisks correspond to the point of closest approach in those cases in which the ellipses failed to intersect.^c

$q^2 (\text{f}^{-2})$	F_{1n}^J	F_{1n}	F_{2n}^J	F_{2n}
5.1	0.16	0.09	0.76	0.75
10.0	0.12	−0.09*	0.49	0.38*
11.5	0.03	−0.11*	0.46	0.34*
15.0	0.18	−0.08*	0.40	0.28*
18.0	0.25	−0.02	0.40	0.28
21.0	0.17	0.00	0.33	0.22

^a See reference 4 and reference 45.

^b See reference 40.

^c See reference 46.

deuteron wave functions, especially in the sense of a comparison of the inelastic scattering cross section near threshold with the elastic scattering cross section. It was in fact demonstrated in Sec. III that the use of wave functions corresponding to a repulsive-core interaction between the neutron and proton for both the free and the bound states permitted one to fit both cross sections simultaneously, thereby removing the discrepancy between the simple Jankus theory⁸ and experiment noted by Kendall *et al.*¹⁰

ACKNOWLEDGMENTS

The author would like to thank I. Cole and E. Windschauer for their computational assistance.

APPENDIX

In this Appendix, we will indicate the none-too-obvious origin of the approximate expressions for the function $M(p, q)$, Eq. (15.2), used in Secs. II and V. We will assume, in accord with the work of Bertocchi *et al.*,³⁴ that the deuteron S -state wave function $u(r)$ can be written in the form

$$u(r) = N \int_0^\infty \rho(z) e^{-zr} dz, \quad (\text{A.1})$$

where for a superposition of Yukawa potentials with a minimum decay parameter λ ,

$$\rho(z) = \delta(z - \alpha) - 2z\sigma(z)\theta(z - \alpha - \lambda), \quad (\text{A.2})$$

and $\sigma(z)$ is the weight function which appears in Eq. (75). The function $F(\theta)$, Eq. (15.4), which corresponds to such a wave function is given by

$$F(\theta) = N \int_0^\infty \rho(z) [z^2 + p^2 + \frac{1}{4}q^2 - \mathbf{p} \cdot \mathbf{q}]^{-1} dz. \quad (\text{A.3})$$

This function has precisely the same structure as the relativistic momentum space wave function $D(t)$,

Eq. (80). In accordance with the discussion of Sec. IVb, q^2 is to be equated to the square of the electron 4-momentum transfer, \mathbf{q} is the 3-momentum transfer in the center-of-mass system of the outgoing nucleons, and \mathbf{p} is the momentum of the proton in that system. Specializing to the case $|\mathbf{p}| = |\frac{1}{2}\mathbf{q}|$, $q^2 = q^2$, which is characteristic of the quasi-elastic peak in the cross-section $d^2\sigma/(d\Omega_e dE_e')$, and calculating $M(p, q)$ using the formula of Eq. (15.2), we obtain

$$\begin{aligned} M(p, q) &= (N^2/q^2) \int_0^\infty \rho(z) dz \int_0^\infty \rho(z') dz' \\ &\quad \times \frac{1}{z^2 - z'^2} \ln \left[\frac{z^2(z'^2 + q^2)}{z'^2(z^2 + q^2)} \right], \quad (\text{A.4}) \\ &= (N^2/q^2) \int_{-1}^1 du \int_0^\infty \rho(z) dz \int_0^\infty \rho(z') dz' \\ &\quad \times \{ [z^2(1+u) + z'^2(1-u)]^{-1} \\ &\quad - [z^2(1+u) + z'^2(1-u) + 2q^2]^{-1} \}, \quad (\text{A.5}) \\ p &= \frac{1}{2}q. \end{aligned}$$

The first term in (A.5) involves q only in the external factor (N^2/q^2) , while the second term involves an extra factor of q^2 in the denominator and consequently vanishes more rapidly for $q^2 \rightarrow \infty$. In fact, when q^2 is larger than the maximum value of z^2 for which $\rho(z)$ is appreciable in magnitude, the second term may be expanded in powers of $[z^2(1+u) + z'^2(1-u)]/(2q^2)$. Using the condition

$$\int_0^\infty \rho(z) dz = 0 \quad (\text{A.6})$$

which corresponds to $u(0) = 0$, one obtains for the leading contribution to the second term

$$\begin{aligned} &\int_{-1}^1 du \int_0^\infty \rho(z) dz \int_0^\infty \rho(z') dz' \\ &\quad \times [z^2(1+u) + z'^2(1-u) + 2q^2]^{-1} \\ &\quad \rightarrow \frac{1}{3q^6} \left[\int_0^\infty \rho(z) z^2 dz \right]^2, \quad q^2 \rightarrow \infty. \quad (\text{A.7}) \end{aligned}$$

For a Hulthén wave function, this becomes essentially $\beta^4/(3q^6)$, a number which is to be compared with the estimate $1/\alpha^2$ for the first term in (A.5). Thus even for $q \approx \beta = 1.43 \text{ f}^{-1}$, the contribution to $M(p, q)$ of the

second term in (A.5) is small, being roughly -1% of the first term. The approximate value of $M(p, q)$ used in Secs. II and V is obtained by dropping the second term in (A.5) altogether,

$$\begin{aligned} M(p, q) &\rightarrow (N^2/q^2) \int_{-1}^1 du \int_0^\infty \rho(z) dz \\ &\quad \times \int_0^\infty \rho(z') dz' [z^2(1+u) + z'^2(1-u)]^{-1}, \\ p &= \frac{1}{2}q, \quad q^2 \rightarrow \infty. \quad (\text{A.8}) \end{aligned}$$

The result given for $M(p, q)$ in Eq. (31) is obtained immediately by taking the $\rho(z)$ appropriate for a Hulthén wave function, $\rho(z) = [\delta(z-\alpha) - \delta(z-\beta)]$. The approximation is excellent for $q > 2$ for both the Hulthén and repulsive core wave functions discussed in the text. Thus, for the Hulthén wave function, and $q = 1, 2, 3, \infty \text{ f}^{-1}$, we obtain for $(q^2/N^2)M(p, q)$ the values 15.262, 15.464, 15.473, and 15.475 f^2 ; the corresponding numbers for the repulsive core wave function are 15.503, 15.668, and 15.669 and 15.671 f^2 .

Approximations for $M(p, q)$ for $p \neq \frac{1}{2}q$ may be constructed by similar methods. The most useful result, that which describes the shape of the central region of the quasi-elastic peak, $p \approx \frac{1}{2}q$, is obtained simply by replacing the denominator in (A.8) by

$$[z^2(1+u) + z'^2(1-u) + 2p^2 + \frac{1}{2}q^2 - 2p|\mathbf{q}|];$$

the external factor N^2/q^2 must simultaneously be changed to $N^2/(2p|\mathbf{q}|)$. This approximation is valid for $(p - \frac{1}{2}q)^2 \ll \lambda^2$, where λ is the minimum decay parameter for the Yukawa potentials.

We remark finally that the matrix element $\langle 1/p \rangle$ defined by Goldberg⁴⁰ in the last paragraph of his paper on the impulse approximation for inelastic electron-deuteron scattering is given to within trivial factors by the integrals in (A.8):

$$\begin{aligned} \langle 1/p \rangle &= \int |\phi(p)|^2 p^{-1} d^3p \\ &= \frac{N^2}{\pi} \int_{-1}^1 du \int_0^\infty \rho(z) dz \\ &\quad \times \int_0^\infty \rho(z') dz' [z^2(1+u) + z'^2(1-u)]^{-1}, \quad (\text{A.9}) \end{aligned}$$

where

$$\phi(p) = (2\pi)^{-3} \int e^{-i\mathbf{p} \cdot \mathbf{r}} u(\mathbf{r}) d^3r. \quad (\text{A.10})$$